Centre for Geo-Information

Thesis Report GIRS-2007-12

Use of high-resolution X-band weather surveillance radar for areal rainfall estimation

Zahra Toofani Nejad

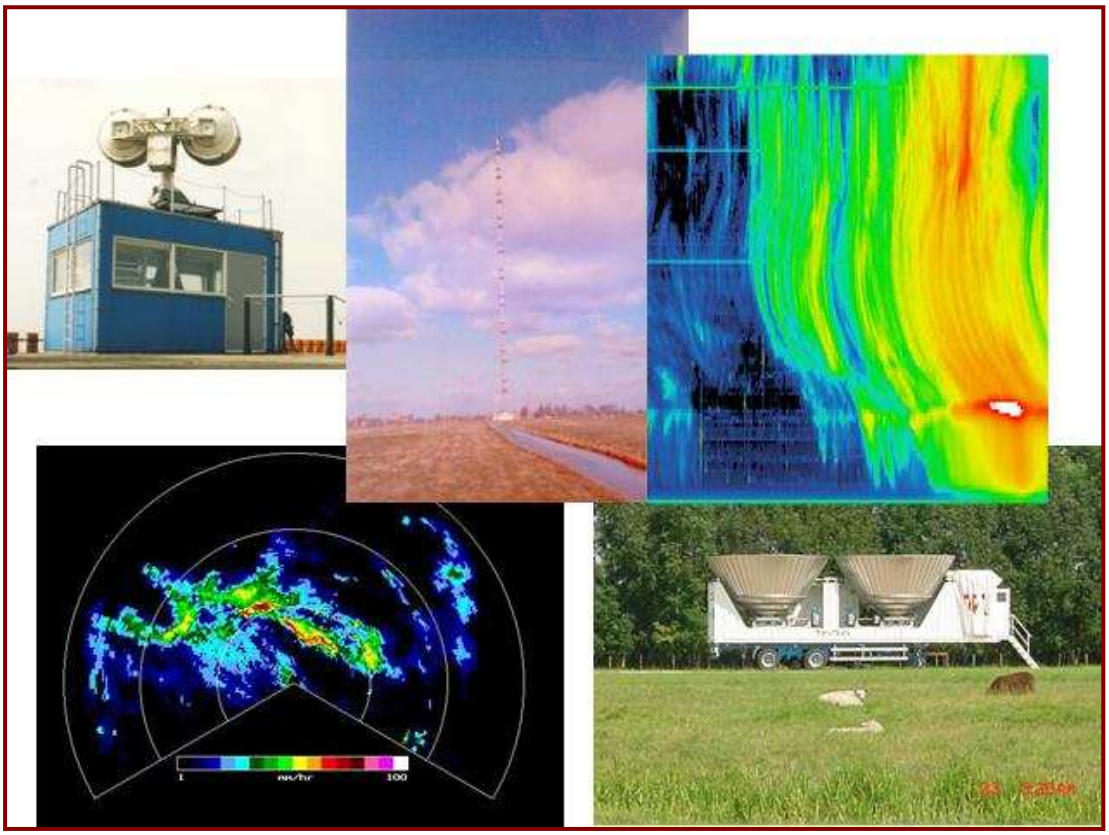

May 2007

WAGENINGEN UNIVERSITY
WAGENINGEN UR

Use of high-resolution X-band weather surveillance radar for areal rainfall estimation

Zahra Toofani Nejad

Registration number 780919838010

Supervisors:

Ir. Hidde Leijnse
Prof. dr. ir. Remko Uijlenhoet
Prof. Dr. sc. nat. Michael Schaepman

A thesis submitted in partial fulfillment of the degree of Master of Science
at Wageningen University and Research Centre,
The Netherlands.

May 2007
Wageningen, The Netherlands

Thesis code number: GRS-80436
Thesis Report: GIRS-2007-12
Wageningen University and Research Centre
Laboratory of Geo-Information Science and Remote Sensing

Acknowledgement

I am very grateful, deep down in my heart, what God has done in my life.

This thesis report represents the result of my student thesis research that is part of the MSc. Geo-Information Science.

First of all, I like to sincerely thank my dear husband, Majid for his loving support and encouragement provided throughout my study, which made me capable of finishing my MSc.

I would like to express my profound gratitude to my supervisors; Prof. Remko Uijlenhoet (Hydrology and Quantitative Water Management group) and Prof. Michael Schaepman offered me the opportunity to perform this research project and improved my understanding concerning radar. I am deeply indebted to Ir. Hidde Leijnse, another supervisor, for several technical support and advice throughout the period of my work. I would like to thank Ir. Remco van de Beek for giving me the initial idea of the thesis. I would like to thank Dr. Herman Russchenberg (TU Delft) for providing the data.

It was my good time that I had to spend 7 months on this thesis. Most of the things were new and challenging for me. I have learned many things from this thesis. And I realized that writing this thesis report was not easy for me at all. But it is worth learning, isn't it?

Zahra Toofaninejad

Wageningen, May 2007

Abstract

Obtaining reliable precipitation observations is important for hydrological simulations and weather forecasting. The most obvious way of measuring rainfall is using by rain gauges. This instrument has been used for many years and has been found to be very accurate at point scale. Knowing rainfall at one point can be useful, but knowing area averaged amounts is more useful. One way to achieve this is by using radar. Radar data can provide insight in the spatial variation of precipitation and can also detect large areas of rain and estimate rainfall rates. These rates can then be used to calculate total amounts of precipitation for a given area. Of course, the radar does not record precipitation directly; instead it processes a returned reflectivity from the precipitation droplets in the volume of the radar beam. The accuracy of radar estimation can be limited at times (Windsor, 2005). Also radar rainfall estimation can be prone to errors because of attenuation and ground clutter. Therefore, the main problem is how those errors can be detected and removed as much as possible from the radar observations (Borga and Fattorelli, 2002).

Weather radar systems nearly always operate in S-, C- or X-band. Since X-band systems require smaller antennas than those at C- or S- band, they are particularly suitable for monitoring small hydrological working (Matrosov et al. 2002, Rahimi et al., 2005).

This report discusses the potential of X-band radar systems for rainfall estimation over an urban area in the Netherlands. It focuses on removing ground clutter and attenuation from X-band radar measurements. In this study measurements from radar are compared against measurements from 4 tipping bucket rain gauges for a rainfall event.

In order to improve rainfall estimation using weather radar, firstly, errors caused by ground clutter and attenuation need to be removed. After that the corrected radar reflectivity value can be converted to rainfall rate via an adequate relationship. To assess the uncertainty in rainfall estimation, the results of estimation have been compared against rainfall rates recorded by rain gauges.

In general, the analysis demonstrated that the radar follows the general trend of the rain gauge measurements but the radar measurements need to be calibrated and corrected for errors. When corrections are applied, results are comparable to the rain gauge measurements. The advantage of radar data compared to rain gauge data is that the radar data can provide much more insight into the spatial variation of rainfall.

Table of Contents

List of Figures

List of Tables

Chapter 1

General Introduction

1.1 Context and background

In many hydrological applications, rainfall estimation over a catchment area is a key issue (Chua and Bras, 1982; Lombardo et al., 2006). In fact, rainfall is the main source of water for hydrological processes. Accurate and reliable measurements of the spatial and temporal distribution of rainfall are very important in hydrology (Vaes et al., 2001, Uijlenhoet, 2001; Tilford et al., 2002, Gray and Laesen, 2004; Cluckie et al, 2005; Uijlenhoet et al, 2006,).

Rainfall is measured using three types of sensors: rain gauge, satellite and ground-based weather radar. Rain gauges are the traditional instruments used for the recording of rainfall and are often regarded as being the “truth”, or reference, for rainfall estimates at ground level (Piman et al, 2007; Wesson et al, 2006). Rain gauges have the advantage of being relatively inexpensive and of providing a direct estimate of the accumulated rainfall at a particular point. However, there are various disadvantages associated with rain gauges. They tend to underestimate during heavy rainfall periods (Wilson and Brandes, 1979) and by providing a point estimate they can fail to capture the spatial variability of rainfall. Of course, inaccurate rainfall estimates based on rain gauges are due to inadequate spatial coverage or configuration

and inadequate gauge density (Borga, 2002). Satellites are an attractive alternative to observe rainfall at global scale from space with coarse spatial and temporal resolution. However, it is difficult to apply satellite rainfall in small scale basins (less than 10^3 km^2) and in real time operation (Linsley et al., 1988; Collier, 1996). In addition to that, the accuracy of satellite rainfall estimation decreases when the time scale is reduced (i.e., from monthly to daily to sub-daily). Weather radar overcomes some of the disadvantages associated with rain gauges and satellites as it provides a rain field with high spatial and temporal resolution and large areal coverage.

Remote sensing of rainfall using ground-based radar is a technology which has been in continuous development since World War II. Application of radar measured rainfall in hydrological and environmental modeling, including real-time hydrological forecasting, has become an active area of research by hydrologists (Collinge and Kirby, 1987; Bell and Moore, 1998, Sun et al., 2000; Borga et al. 2000; Jordan et al., 2000; Borga et al, 2004; Osrodka et al., 2004; Jordan et al., 2004; Lopez et al., 2005; Berne et al., 2006).

In this context, weather radars have several advantages, since a single site is capable of obtaining coverage over a vast area with high spatial-temporal resolution, and the radar rainfall products are crucial for input to runoff and flood forecasting models and for statistical characterization of extreme rainfall frequency (Uijlenhoet, 1992, Uijlenhoet, 2001, Krajewski and Smith, 2002; ten Heggeler, 2004; Osrodka et al., 2004). But rain fields estimated from weather radars experience various data quality problems such as ground clutter, anomalous propagation and beam blocking, to name a few (Lombardo et al., 2006). Another disadvantage of weather radars is that they provide an indirect measurement of precipitation intensity, so the returned power of measured reflectivity values (Z) has to be converted to rain-rate (R) by an appropriate transformation, such as the Marshall Palmer relation (Marshall and Palmer, 1948). Hence the accuracy of the estimation of Z−R relationships is important (Rosenfeld et al., 1993; Collier, 1996). The true radar reflectivity may be determined based on the Drop Size Distribution (DSD) of rainfall and is related with rainfall intensity to estimate the true Z−R relationship (Battan, 1973). However, unavailability of raindrop size distribution information restricts the determination of an accurate Z−R relationship and variations in the DSD may cause additional uncertainties in the retrieved R.

Calheiros and Zawadzki (1987) applied a regression analysis technique to determine the relationship of synchronous datasets between measured rainfall intensities by rain gauges and measured or effective reflectivities by weather surveillance radar at the pixels over the rain gauges. However, in reality perfect synchronization between Z and R is unachievable, except at the closest range and nearest to the ground. The non-synchronous Z−R pairs are due to: 1) the large discrepancy between the sample volume of the rain gauge and the radar, 2) timing and geometric mismatches, and 3) the large variability of the Z−R relationships mainly due to differences of rainfall characteristics, locations and times i.e. DSD variability (Battan, 1973; Uijlenhoet, 2001). These problems reduce the accuracy of Z−R conversion and hence of radar rainfall estimates.

Recently, there has been an increased interest in radars operating at short wavelengths; roughly from 1 to 5 cm. Examples are X-band radar networks and K-band radars operating from spaceborne platforms (e.g., the Tropical Rainfall Measuring Mission (TRMM) and Global Precipitation Measurement (GPM) satellites).

At such wavelengths the raw radar data is prone to various sources of error and thus has to be filtered before further processing. One of the sources of error is clutter. Clutter is unwanted signals, resulting from e.g. reflections at non–meteorological obstacles such as mountains, buildings, and industrial plants (ground clutter), or from birds and airplanes (moving clutter) (Chrisman et al., 1995, Gerstner et al., 2002, Ramirez et al., 2005, Lombardo et al. 2006). Such obstacles alter the signal not only at their location, but also behind them with respect to the position of the antenna. The basic way to filter the ground clutter is to record the measured signals on a dry day in a so- called clutter map. The clutter map is subtracted from the operationally measured signals. Thereby, each measured reflectivity value is compared to its corresponding value on the clutter map. Values with precipitation are reduced if they are assumed to be contaminated by clutter (Gerstner et al., 2002, Ramirez et al., 2005).

Another source of error in this field that must be corrected is attenuation by rain. When hydrometeors reflect the energy of the pulse sent by the antenna, they also weaken the incoming pulse for the following volumes (Berne and Uijlenhoet, 2006).

The attenuation of a radar signal at short wavelengths is a serious problem meteorologist and hydrologists are facing. In heavy rain, reflectivity information can be completely lost from large portions of a radar scan. Thus the attenuating wavelengths appear to be of limited applicability in rain measurement; in addition, attenuation substantially reduces the sensitivity for the detection of precipitation viewed through intervening rain (Hitschfeld and Bordan, 1953). This is due to the increase in attenuation at higher frequencies, whereas at S- and C- bands the attenuation of the radar signal is assumed to be negligible.

X-band radars operate at a wavelength of 2.5-4 cm (a frequency of 8-12 GHz). Because of the smaller wavelength, the X band radar is more sensitive and can detect smaller particles. These radars are used for studies on cloud development because they can detect the tiny water particles and also used to detect light precipitation such as snow. Since X-band systems require smaller antennas than those at C- or S- band, they are particularly suitable for monitoring small hydrological catchments (Matrosov et al. 2002, Rahimi et al., 2005). Attenuation is a major problem at X-band and must be corrected for, if reflectivity values are to be used to estimate rainfall (Park et al., 2004; Berne and Uijlenhoet, 2006). Hitschfeld and Bordan (1954) demonstrated that their forward-correction algorithm is inherently unstable and concluded that some constraint on the total attenuation is required. The possibility of obtaining X-band attenuation from the difference between S- and X-band reflectivity has been reconsidered recently by Perez and Zawadzki (2003), who showed that, in rain with reflectivity greater than 40 dBZ, attenuation behaves very similarly to reflectivity and therefore provides little additional information.

1.2 Research Objective and Research Questions

This report deals with a study to explore the potential of X-band radar systems for rainfall estimation over an urban area in the Netherlands. This work focused on removing ground clutter and attenuation from X-band radar measurements. In this study measurements from the X-band FM-CW weather surveillance radar SOLIDAR are compared against measurements from 4 tipping bucket rain gauges for a rainfall event that occurred on December 19, 1991.

In order to achieve the objective, the following research objectives and questions are defined:

1. How to improve rainfall estimations using weather radar?
2. How to assess the uncertainty in rainfall estimation?

In order to improve rainfall estimation using weather radar, firstly, errors caused by ground clutter and attenuation need to be removed. After that the corrected radar reflectivity value can be converted to rainfall rate via an adequate relationship. This study did not focus on an improvement of the Z-R relationship. Results from literature have been used. To assess the uncertainty associated with rainfall estimation, the results of the estimation have been compared against rainfall- rates recorded by rain gauges.

1.3 Thesis structure

This thesis is divided into 4 parts as follows:

Chapter 2 gives a short introduction about the principle of weather radar, its major sources of error and the characteristics of the SOLIDAR radar.

Chapter 3 deals with methodology, study area and input data.

In Chapter 4, the results of the ground clutter map, the corrected radar reflectivity and the results of the comparison are presented and discussed.

In the last chapter the conclusions are drawn and recommendations for further study are discussed.

Chapter 2

Principles of Weather Radar

2.1 Introduction

RADAR stands for "RAdio Detection And Ranging". The RADAR sensor transmits a microwave (radio) signal towards the target and detects the backscattered portion of the signal. The strength of the backscattered signal is measured to discriminate between different targets and the time delay between the transmitted and reflected signals determines the distance (or range) to the target. Because it transmits pulses of microwave electromagnetic radiation this type of instrument is classified as an "active sensor".

In application of RADAR for rainfall estimation, the scattering medium is considered to be rainfall and the scatterers are raindrops. However, radar does not provide direct measurements of rainfall, but only indirect ones via the interaction of radio signal with raindrops. The radio signal received by the raindrops is scattered back into the direction of the radar and received by its antenna. This is visualized in figure. 1.

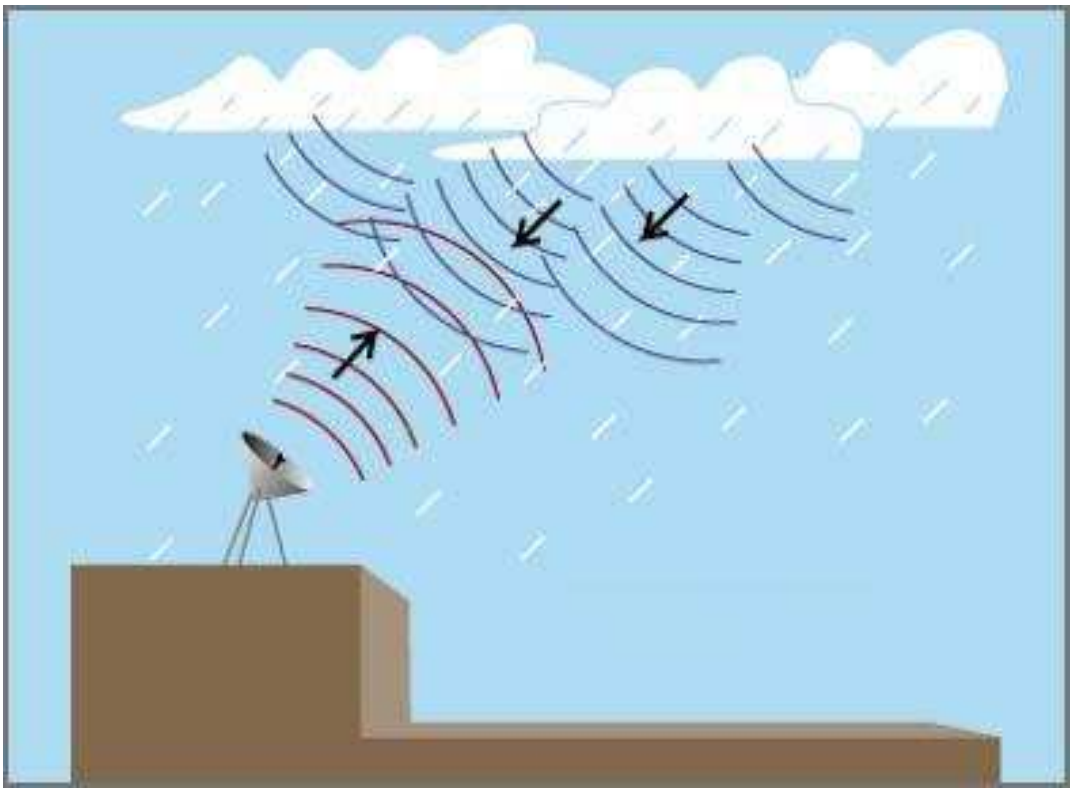

Figure 1: Principle of the operation of weather radar. The radar sends out a signal, which is then reflected back to the radar by raindrops.

The fundamental radar equation describes the received power from raindrops as function of the characteristics of the radar and properties of the objects. It can be written as (Uijlenhoet, 1992):

$$P_r(r) = \frac{C}{r^2}.|K^2|.L^2(r).Z(r) \qquad (1)$$

where P_r : The average power received by radar[W],

C: The radar constant [W],

r: The distance of the object from the radar [m],

L^2: The signal (two- way) attenuation factor,

Z: Radar reflectivity factor [mm^6*m^{-3}] and

$|K|^2$: A coefficient related to the dielectric constant of water.

The signal (two- way) attenuation factor (L^2) is related to twice the specific attenuation coefficient (k [$dB*km^{-1}$]) integrated over the range s [km] from zero to r.

In contrast to S- or C-band, Radar reflectivity factor depends on the radar wavelength at X-band.

Because in practice the variations in radar reflectivity may span several orders of magnitude, it is often convenient to use a logarithmic scale. The logarithmic radar reflectivity is defined as $10*\log_{10}(Z)$ and is expressed in units of dBZ (e.g. Battan, 1973).

If it is assumed that all raindrops in the measurements volume scatter independently both the radar observation (Z) and rain rate (R) can easily be expressed in terms of integrals over the raindrop size distribution (DSD) (Uijlenhoet, 1992, Uijlenhoet, 2001, Tristan and Graeme, 2002, Uijlenhoet et al., 2006, Berne and Uijlenhoet, 2006).

A general form of DSD (the gamma DSD) has been reported by Uijlenhoet (1992):

$$N(D) = N_0 * D^{\alpha} * \exp(-\Lambda * D) \quad ; \quad D_{\min} \le D \le D_{\max} \tag{2}$$

where N(D): The raindrop size distribution [$mm^{-1}m^{-3}$]

N_0 : The normalization factor [$mm^{-(1+\alpha)}*m^{-3}$],

D: The spherical raindrop diameter [mm],

α : The shape parameter and

Λ : The scale parameter [mm^{-1}].

Many radar algorithms assume the Marshall- Palmer raindrop size distribution (N_0=8000, $\Lambda = 4.23R^{-0.21}$ and α =0) to obtain relations of the form R-Z and Z-*k* which are directly invertible to obtain rain rate given radar reflectivity measurements. These methods have the advantage that they solve the problem into a simple analytical form, which results in a computationally quick and relatively simple retrieval algorithm (Tristan and Graeme, 2002).

Use of a Z-*k* relationship allows us to consider the range profile of the specific attenuation coefficient *k*(r) as being the only unknown quantity in the radar equation. Thus, radar measurements are firstly used to correct the measured Z-profile for attenuation. Then the rain- rate profile is obtained by using a relevant frequency-dependent R-Z relation.

The link between Z and the rain rate R is called Z– R relationship and depends on the unknown drop size distribution within the measured volume. Most publications use an empirical equation for R-Z relationship of the form

$$Z=aR^b \quad (3)$$

Where the values of a and b vary per location, per event and even within events, but they are independent of R [mm h^{-1}]. Of course they are dependent on the raindrop size distribution (Sempere-Torres et al., 1998, Tristan and Graeme, 2002, ten Heggeler, 2004). The famous R-Z relationship that was proposed by Marshall and Palmer (1948) and corrected by Marshall et al. (1955) is widely used:

$$Z=200R^{1.6} \quad (4)$$

2.2 Sources of error

The error sources associated with radar rainfall observation considerably reduce the accuracy and reliability of the radar derived rainfall data. The most important of them are:

- **Uncertainty in radar calibration:** Radar system can be affected by calibration errors. If a radar system is not well calibrated, then the measured powers do not correspond to the actual powers. This will introduce a bias in the radar power measurements which may greatly affect the corresponding rainfall estimates.

- **Errors associated with ground clutter:** As mentioned before the ground clutters are unwanted signals. Because of ground clutter, rainfall rate estimation algorithms may give non zero rainfall intensity values even there is no rain when clutter is present. Several methods have been developed to correct this error.

- **Errors associated with attenuation:** attenuation is the reduction of the intensity of the electromagnetic signal along its path as a result of the absorption and scattering of the signal by atmospheric gasses and hydrometeors. Because of the reduction of energy along the path of the signal

(i.e. attenuation) the received echo can be reduced by as much as an order of magnitude.

- **Uncertainty in the Z -R relationship:** Errors can occur because the exact size distribution of all droplets inside the sample volume of the radar is unknown. If one wants to find the best relationship, it is necessary to know the actual DSD, which is practically impossible.
- **Other error sources:** Errors caused by temporal sampling, spatial sampling, and height sampling will remain, even after other sources of error have been removed. Because they cannot be easily reduced or removed, these errors affect the accuracy of rainfall measurements.

2.3 SOLIDAR radar

The radar data used in this study are from SOLIDAR, which is an X-Band FM-CW (Frequency Modulated Continuous-Wave) Solid-State Weather Surveillance Radar and was located on the roof of the Faculty of Electrical Engineering of Delft University at a height of approximately 100 m above ground level (figure 2). The radar beam of SOLIDAR has an elevation of 1.7 ° and a range and azimuth resolution after preprocessing of 120 m and 1.875 °, respectively. Specifications of the radar are given in Tables 1 and 2. This radar was built to gain knowledge about rain cell geometries and rain cell locations during rainfall events. SOLIDAR can be used to estimate the rain intensity up to 15 km away from the radar (for more information about SOLIDAR, see Ligthart and Nieuwkerk, 1990).

Figure 2: The X-band weather surveillance radar, SOLIDAR, which was operated by Delft University of Technology.

Table 1: SOLIDAR hardware specifications.

Radar type	*Linear FM. Sawtooth*
Transmitted power	30dBm
Maximum received Signal level	-17dBm
Center frequency	9.47 GHz
Frequency excursion	5 MHz
Range resolution	30 m
Sweep time	5 ms
Beat frequency max.	102.4 kHz
Antenna gain	38 dB
Beam width	2.8^{o}
Antenna revolution time	15.36 s

Source: Ligthart and Nieuwkerk, 1990

Table 2: SOLIDAR specifications after processing.

Range r_{max}	15.36 km
Range resolution	120 m
Azimuth resolution	1.875^{o}
Number of range cells	128
Number of sector angels	128
Total sector	240^{o}
Minimum detectable rain intensity	1 mm/h
Maximum detectable rain intensity	100 mm/h
Dynamic range ADC	96 dB

Source: Ligthart and Nieuwkerk, 1990

Chapter 3

Methods and Input Data

3.1 Preprocessing of raw data

3.1.1 Ground clutter

Clutter is an unwanted radar return from non meteorological targets. Typically, these clutter targets are stationary, hard targets such as buildings, mountains, towers, etc (Chrisman et al., 1995, Stagliano et al., 2002). Such obstacles alter the signal not only at their location, but also behind them with respect to the position of the antenna (Figure 3). Clutter is more evident when low elevation angles are used since the radar signal travels close to the earth's surface especially at ranges close to the radar (Lombardo et al., 2006).

Elimination of ground clutter is a prerequisite for the use of weather radar, both for quantitative and qualitative purposes. To minimize the errors caused by ground clutter it is necessary to first establish a clutter map. A simple solution for creating a clutter map is the use of a series of radar images in clear sky conditions (e.g. an average ground clutter map). The large and rapid-short term fluctuations of clutter pose a serious problem in the choice of the "rejection-threshold". During extensive

measurements with radar, a threshold should be chosen that eliminates 90% of the ground clutter echoes, regardless of its distribution. Each pixel below the threshold value will be removed and all values that are greater than threshold will be added to the clutter map.

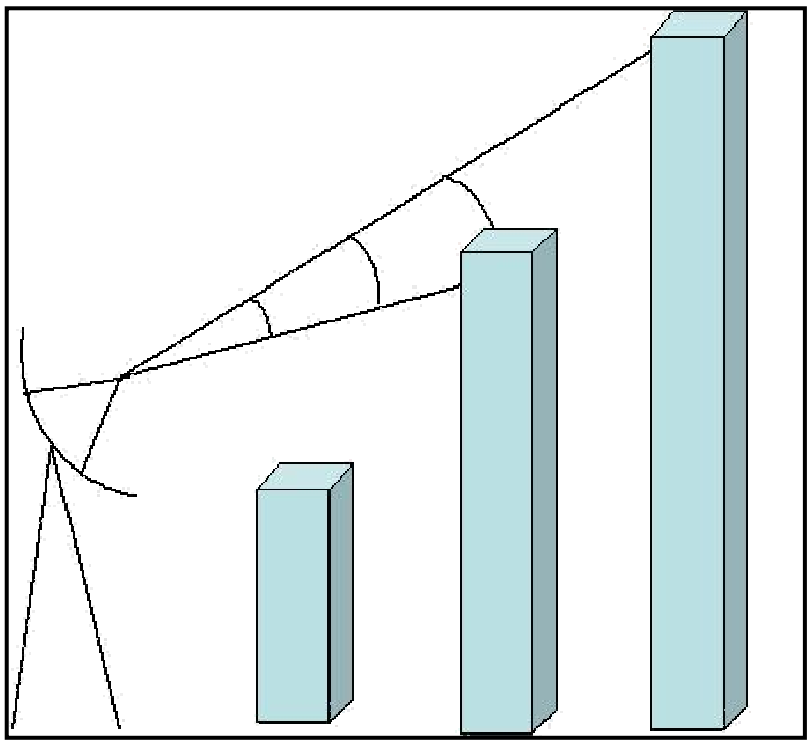

Figure 3: Schematic of ground clutter obstacles which alter the signal at their location and also behind them.

The disadvantage of the clutter map method is obviously residual clutter and the loss of considerable valid precipitation, a compromise that depends on the value of the selected threshold (Gabella and Notarpietro, 2002).

With this clutter map, the ground clutter error can be removed by two methods:

Method 1: Subtracting the clutter map from the raw image.

Method 2: Use of a nearest neighbor window for those locations that are identified as clutter.

The first method is the simplest method. Estimated ground clutter intensities are subtracted from the original image (Gerstner et al., 2002).

The second method disregards any pixels that have been marked as clutter. The values of these pixels are replaced by the averages of neighboring pixels. When the window

is used, the center pixel in the new (filtered) image would be the average value of the 9 pixels in the original image contained in the window at that point (Figure. 4) excluding pixels marked as clutter. Of course the size of the window is dependent on the size of clutter. The size of the window can be increased if the size of the clutter is larger than that of the original window.

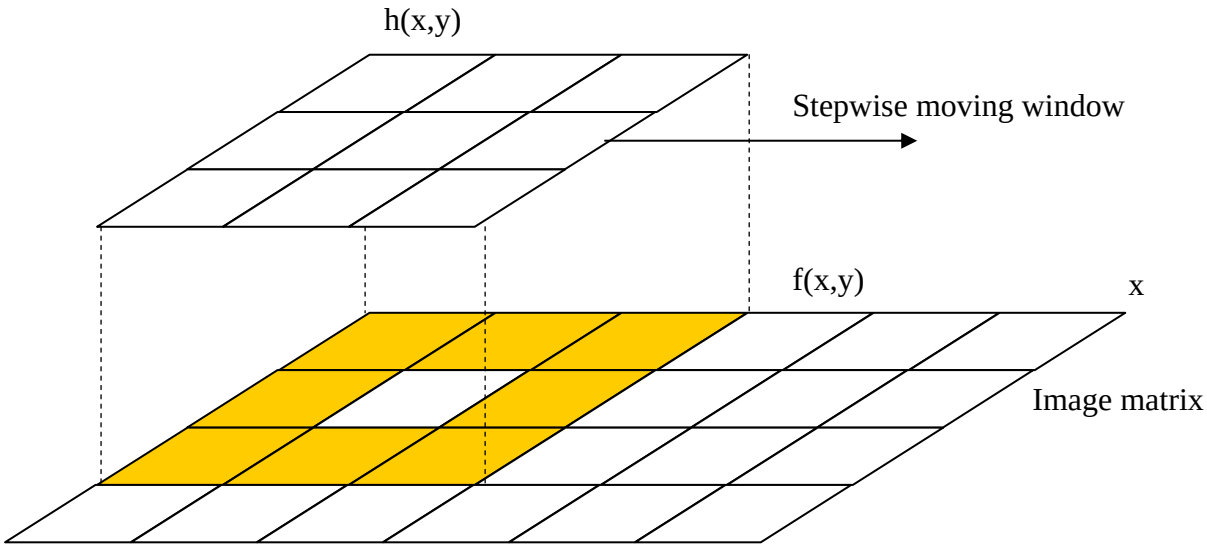

Figure 4: Effect of the window on the original image. *h (r,s)*: ground clutter weight map, *f (x,y)*: original image.

For implementing of this window on the raw image, two points must be assumed (Gerstner et al., 2002):

i) All cells of clutter map will have a weight. The weight of pixel will be 1 if doesn't have clutter and will be 0 if it has a clutter.

ii) The window is moving per clutter. This means that the window will only be applied to the raw image corresponding to the locations on the clutter map. At all locations where clutter was identified the window will be applied.

3.1.2 Attenuation

At short wavelengths, especially X- and K- band, weather radar signals are attenuated by the precipitation along their paths. This is a major source of error for radar rainfall estimation. Attenuating wavelengths thus appear to be of limited applicability in rain measurement; in addition, attenuation reduces very substantially the sensitivity for the

detection of precipitation viewed through intervening rain (Hitschfeld and Bordan, 1953). The reflectivity measured by radar must be corrected for attenuation, in order to improve the accuracy of rainfall estimation (Uijlenhoet, 1992, Park et al., 2004).

A common hypothesis for correction of this error is that the radar reflectivity factor Z and the specific attenuation coefficient *k* for rain may be related through a power- law relationship:

$$k = \alpha Z^{\beta} \tag{5}$$

where the parameters α and β depend on frequency and the DSD (Hitschfeld and Bordan, 1953, Uijlenhoet, 1992, Marzoug and Amayenc, 1994, Uijlenhoet et al., 2006).

The resulting equation is implemented as a recursive correction scheme as follows:

$$Z_{corr,i} = Z_i * f_i$$

$$f_i = 10^{[L\alpha Z_i^{\beta} + \sum_{j=1}^{i-1} 2L\alpha Z_{corr,j}^{\beta}]/10} \tag{6}$$

Where:

Z_i : The raw radar reflectivity in range cell *i*,

$Z_{corr,i}$: The corrected radar reflectivity factor in range cell *i*,

L: Range resolution [km],

α , β : Constant values.

In this approach it is assumed that f_i = 10 if the value of f_i >10. With this additional constraint the algorithm will not become unstable.

3.2 Conversion of reflectivity factor to rainfall rate

The next step after correction is to convert the reflectivity factor to rainfall estimates to compare with the actual rainfall.

As mentioned in the previous chapter the Marshall and Palmer (M-P) relationship has been used in most studies. The M-P Z-R relationship seems to work well for stratiform precipitation in the UK (Harrison et al., 2000), but this relationship may not be adequate for the Netherlands because of variations in the shape of the Drop Size Distribution (DSD). However, it is well known that the Z-R relation in conventional radar produces large errors in rainfall estimation, because of the sensitivity of its coefficients to natural variations of DSD and be cause of ground clutter (Park et al., 2004, Ramirez et al., 2005)

For the SOLIDAR frequency in Dutch conditions, the constant of the power- law Z-R relationship was derived using long term measurements of drop size data (Leijnse,2006, personal communication). The Z-R relationship used in this study is:

$$Z=171R^{1.73} \tag{7}$$

3.3 Radar- gauge comparison over the study area

The purpose of this study is to explain quantitatively the discrepancies between the gauge and radar rainfall amounts. The project used Mean Bias Error (MBE) and the Root Mean Squared Error (RMSE) as comparison factors between rain gauges and radar rain rates.

$$MBE = \frac{\sum_{i=1}^{N_t}(R_i - P_i)}{N_t} \tag{8}$$

$$RMSE = \left[\frac{\sum_{i=1}^{N_t}(R_i - P_i)^2}{N_t}\right]^{0.5} \tag{9}$$

Where:

N_t : The number of time steps in the period of study,

P_i : The rain gauge measurement for the ith time step and

R_i : The radar estimate for the ith time step.

However, radar and rain gauges use fundamentally different methods to estimate rain; rain gauges collect water over a period of time, whereas radar obtains instantaneous snapshots of electromagnetic backscatter from rain volumes that are then converted to rainfall via an algorithm. Rain gauges provide point estimation but radar obtains the volume estimation. Also it is important to remember that radar usually looks above the earth's surface while a rain gauge is located right on the ground (Lombardo et al., 2006).

3.4 Study Area

Measurements from the X-band weather surveillance radar (SOLIDAR), which was operated by Delft University of Technology, are compared against measurements from 4 tipping bucket rain gauges. The event that was used for comparison occurred on December 19, 1991 in the southwestern part of The Netherlands (water board Hoogheemraadschap van Delfland) (Fig. 5). The maximum instantaneous rain rate recorded by one of the gauges is 35 mm h^{-1}. The maximum instantaneous rain rate estimated by radar was approximately 28.2 mm h^{-1}.

The tipping bucket rain gages have receptor areas of about 500 cm^2. They were calibrated in the laboratory and are reported to have resolutions of about 0.2 mm. They are installed in a line configuration in order to be able to investigate the range effects involved in the radar measurements. Some information has been given about the rain gauge sites in the Table 3 (Uijlenhoet, 1992). Fig. 6 shows a tipping bucket rain gauge similar to those installed in the study area. Fig. 7 represents the time series of rain rate from 4 gauge measurements for December 19, 1991.

Each pixel of produced X-band radar image represents 1 value of reflectivity at 1 time step (16s). The rainfall intensity was calculated at each time step and per pixel. Fig. 8 illustrates the radar reflectivity at different time steps.

Figure 5: Map of western part of the Netherlands with maximum range of SOLIDAR X-band weather radar. The four '+' symbols in the first image indicate where the rain gauges were located.

Table 3: Characteristics of the rain gauge locations.

Location	*Gauge*	*Range [m]*	*Azimuth [N]*	*Beam Height [H]*
Vletpoder (W1)	Gauge 2	8864	266.6	359
Van Schie (W5)	Gauge 4	7345	266.6	314
Ammerlaan (W0)	Gauge 1	6276	265.0	282
Zuidgeest (W2)	Gauge 3	8006	262.5	334

Source: Uijlenhoet, 1992

Figure 6: Tipping bucket rain gauge in closed and open position.

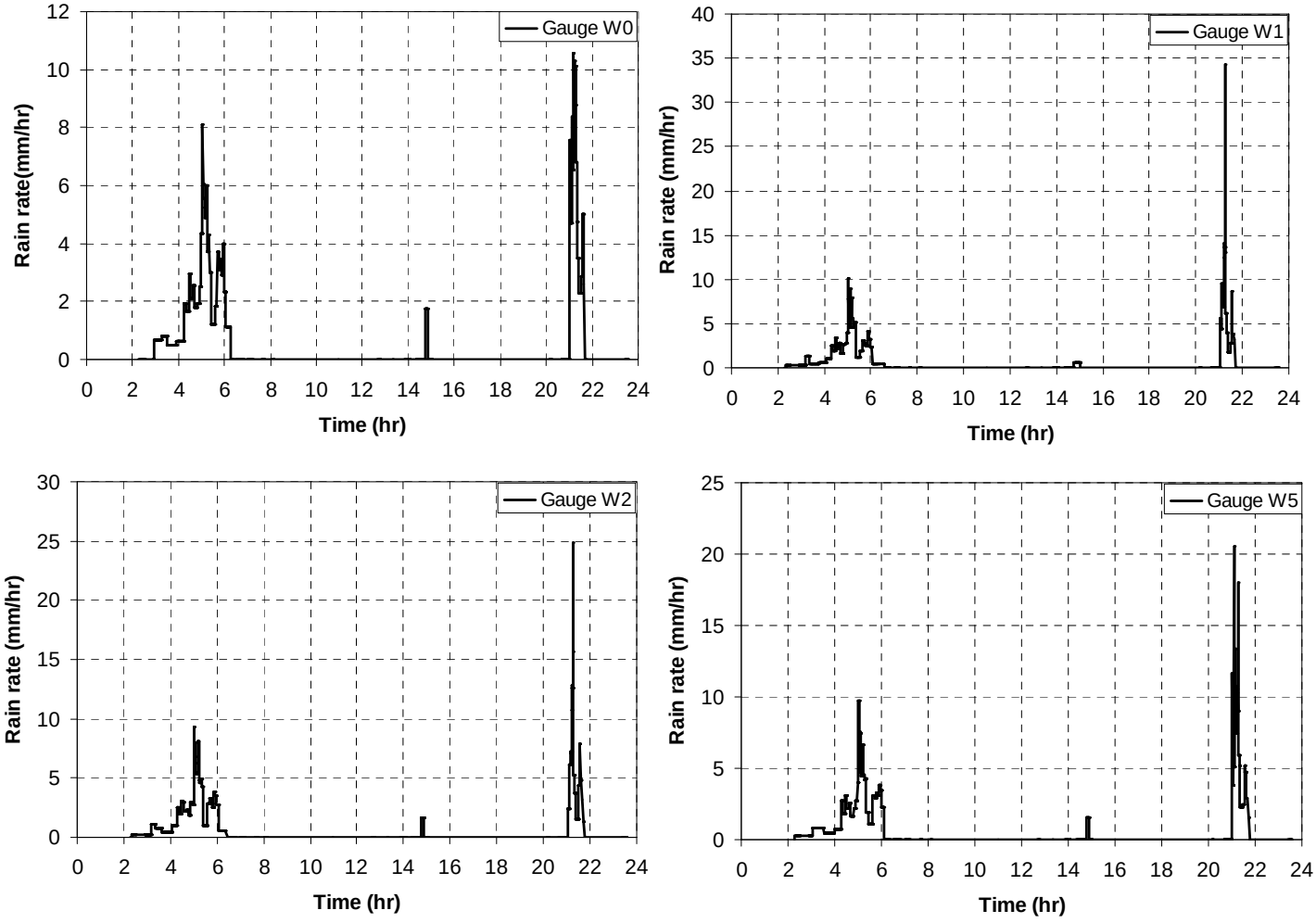

Figure 7: Rain rate from 4 gauge measurements for December 19, 1991.

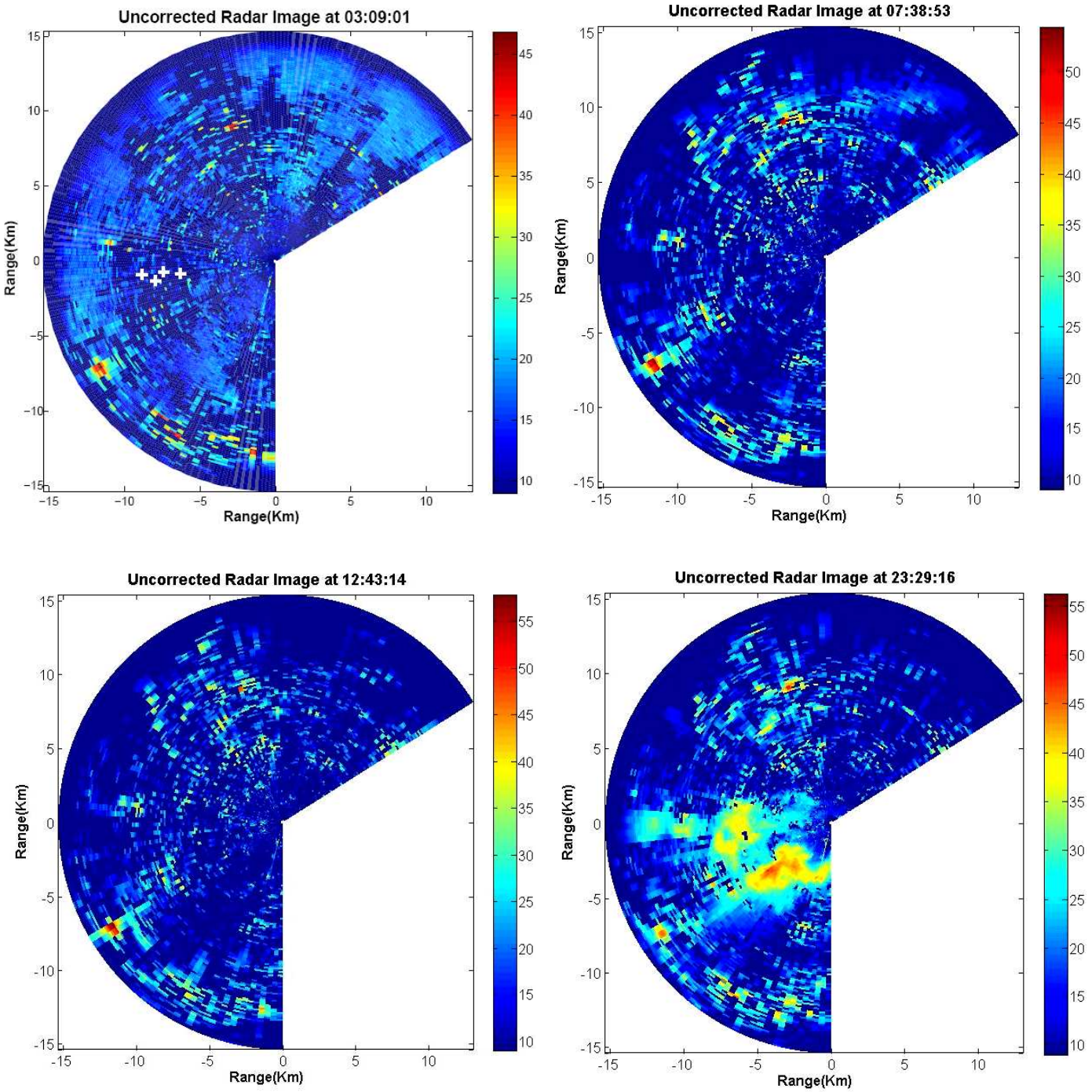

Figure 8: Radar reflectivity at different times on December 19, 1991. The four '+' symbols in the first image indicate where the rain gauges were located.

Chapter 4

Results and Discussion

In order to improve radar rainfall estimation, as the first step, errors caused by ground clutter and attenuation have to be removed. This means that raw weather radar data need some preprocessing before they can be converted into rainfall intensities.

4.1 Preprocessing of X-band radar data

As stated earlier, elimination of ground clutter is a prerequisite for the use of weather radar, both for quantitative and qualitative purposes. Therefore ground clutter errors have to be removed from the raw data. In order to do this, first of all a ground clutter map (GCM) should be made. Since no data have been recorded by the radar during clear sky conditions, two data sets were selected in very light rain to find the ground clutter (as described in the previous chapter). The first 320 time steps were used as one data set and those from 780 up to 1100 were selected as another one. After trial and error the values of 22 dBZ and 25 dBZ were selected as thresholds for each dataset respectively. However, the GCMs that were derived from those data sets were not completely the same. Of course if the value of the threshold of each dataset is increased, the difference between the images becomes smaller, but the apparent ground clutter is decreased as well. Based on visual inspection the second image

(corresponding to the second dataset) was selected as ground clutter map. It is more similar to the site location map than the first image and also according to the second image, the location of each city can be estimated. Fig. 9 the ground clutter map is illustrated; White areas are the clutter and black areas are no clutter.

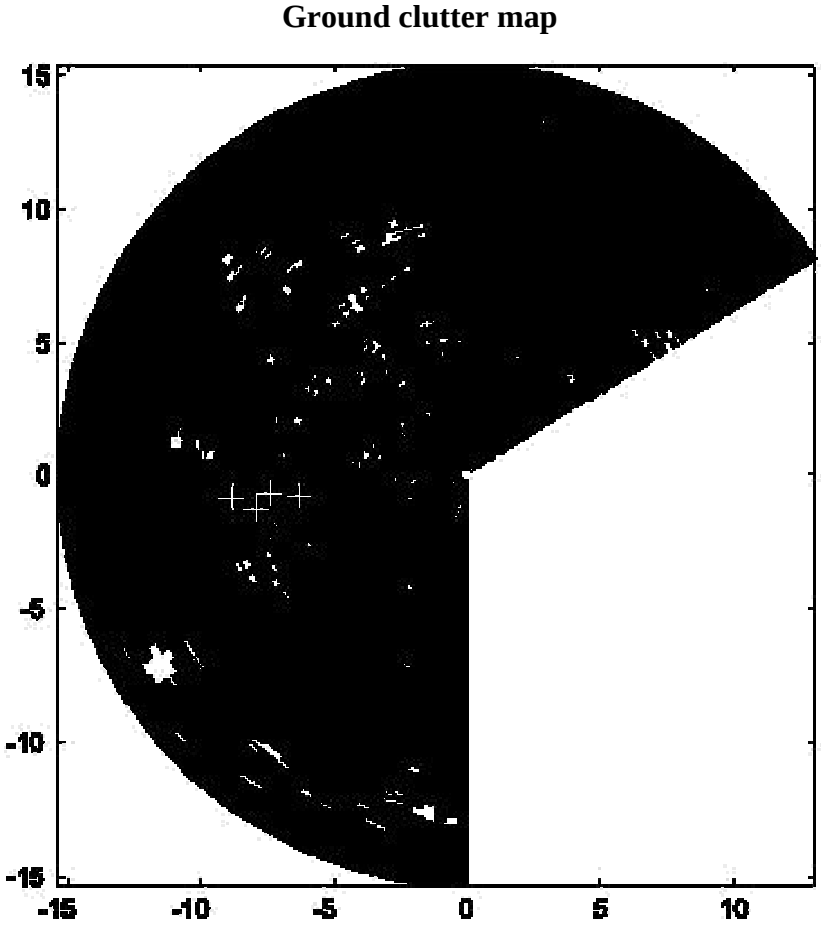

Figure 9: Illustration of location of ground clutter in the study area. White areas are clutter. The '+' symbols in the image indicate where the rain gauges were located.

When the ground clutter map is available, it is easy to apply a clutter correction algorithm. In this study, two methods have been selected for removal of ground clutter (see methodology). After the clutter has been removed, attenuation correction is applied to the radar data according to Eq.6. Figs. 10-12 represent the processes of error correction at different time steps and different clutter correction methods. In each figure, the first image depicts uncorrected radar reflectivity, the second and third image are after clutter correction and the fourth and fifth image present the radar reflectivity image corrected for both clutter and attenuation.

A comparison of the uncorrected image and clutter-corrected image shows some differences. These differences are recognizable by their histograms. As can be seen in fig. 10 the minimum value for radar reflectivity in the un- corrected image is 9 dBZ. For the second image and third image these values are -0.8 and 9 dBZ, respectively. Also, the maximum value of the radar reflectivity in fig. 11 for the first image was 57 dBZ and after clutter correction this value decreased to 48 dBZ.

In the first method of removal of clutter errors, a simple subtraction function was applied, whereas in the second method the effect of neighbor cells has been considered. For the second method a 3*3 window has been selected. Note, however, that the size of the window can be increased according to the sizes of the clutter areas. The advantage of the second method is that it is based only on the location of clutter whereas the first method is based on the location and intensity of clutter. This dependency on the intensity of clutter causes an error itself; because the intensity of clutter can change in different weather conditions. Also it is highly variable in time. For example the reflection from wet buildings is not the same as reflection from dry buildings. Therefore, it is assumed here that the result of the second method of elimination of clutter error is better than the first method.

For better insight, the difference of these two methods has been shown in the Fig. 13 by subtracting the results derived from method one and two. As shown in Fig 13, the pixels values in the first method are higher in the most area.

From the comparison of the clutter-corrected image and the fully (both clutter and attenuation) corrected image in figs. 10 and 11, it can be concluded that the difference between these images is not very large. Therefore it demonstrates that the influence of attenuation is small for the relatively low rain rates during the event considered (Uijlenhoet et al., 1997). In fig. 12, on the other hand, where the rain intensity is higher than at other times, the effects of attenuation correction are clearly illustrated.

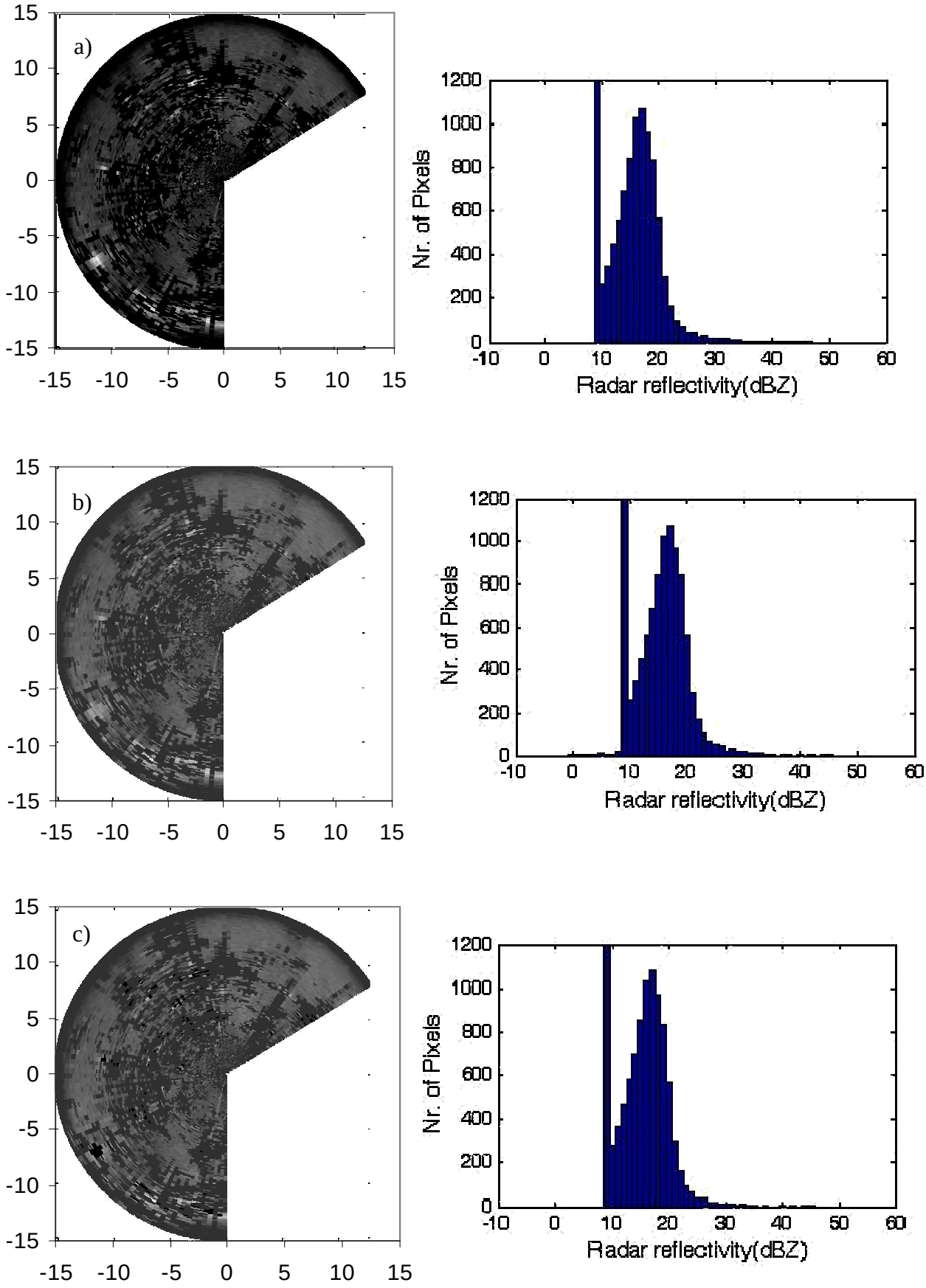

Figure 10: Illustration of preprocessing of radar reflectivity at 03:09:01 on December 19, 1991: a) raw image derived by radar, b, c) clutter corrected image using the first and second method and d, e) final images after removal of attenuation error from images b and c (continued on next page).

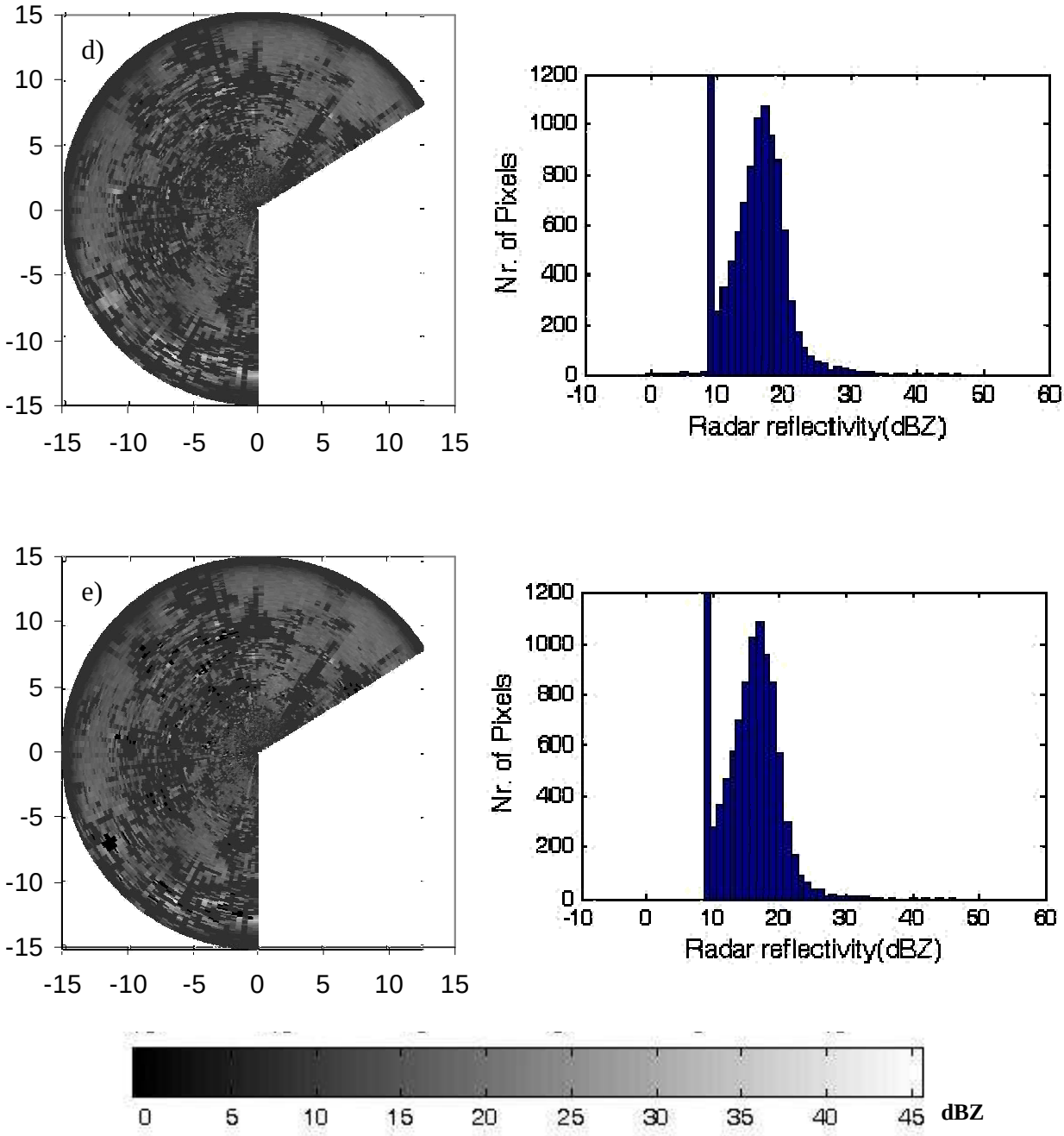

Figure 10 (continued).

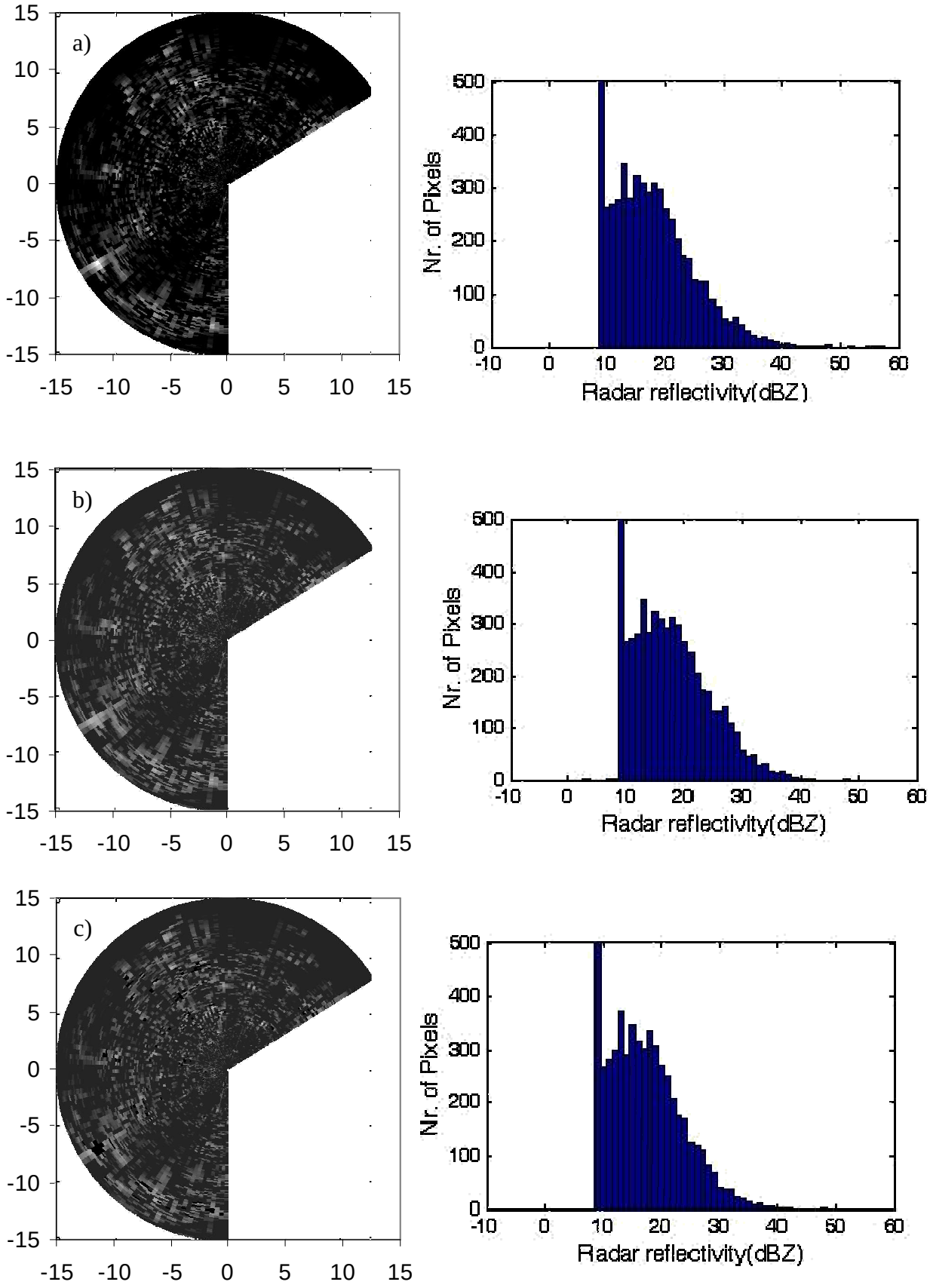

Figure 11: Illustration of preprocessing of radar reflectivity at 12:43:14 on December 19, 1991: a) raw image derived by radar, b, c) clutter corrected image using the first and second method and d, e) final images after removal of attenuation error from images b and c (continued on next page).

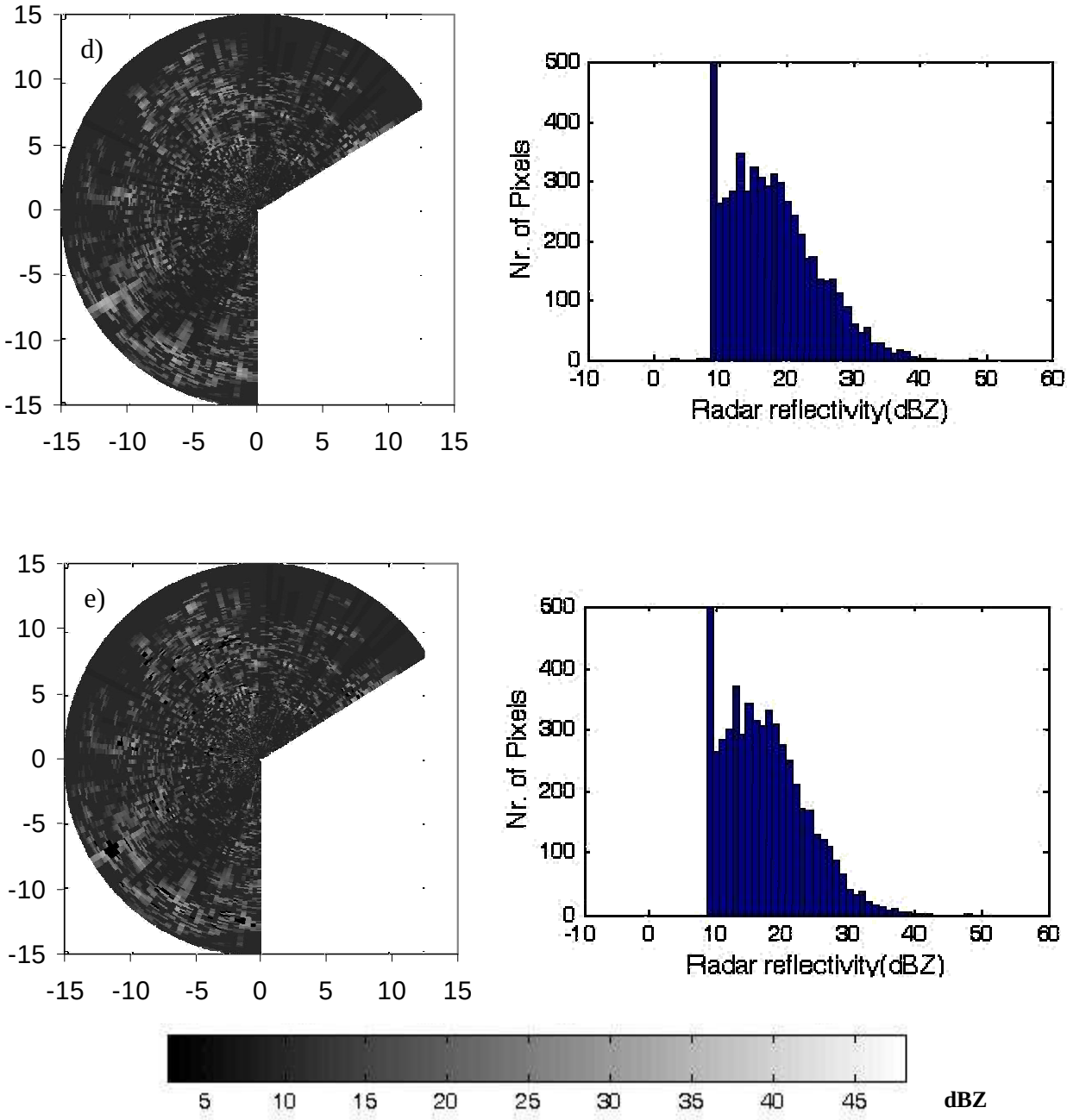

Figure 11 (continued).

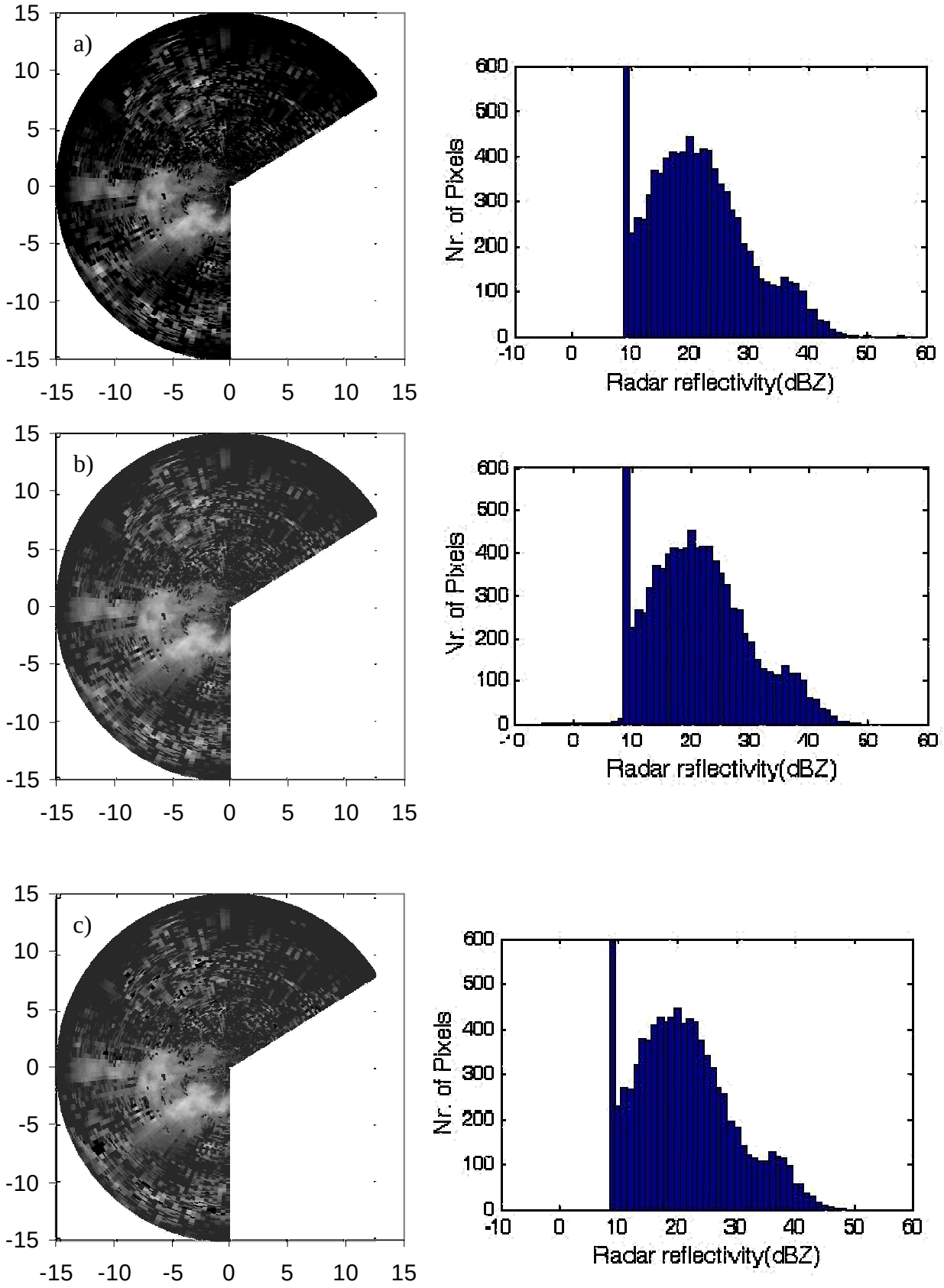

Figure 12: Illustration of preprocessing of radar reflectivity at 23:28:16 on December 19, 1991: a) raw image derived by radar, b, c) clutter corrected image in first and second method and d, e) final images after removal of attenuation error from images b and c (continued on next page).

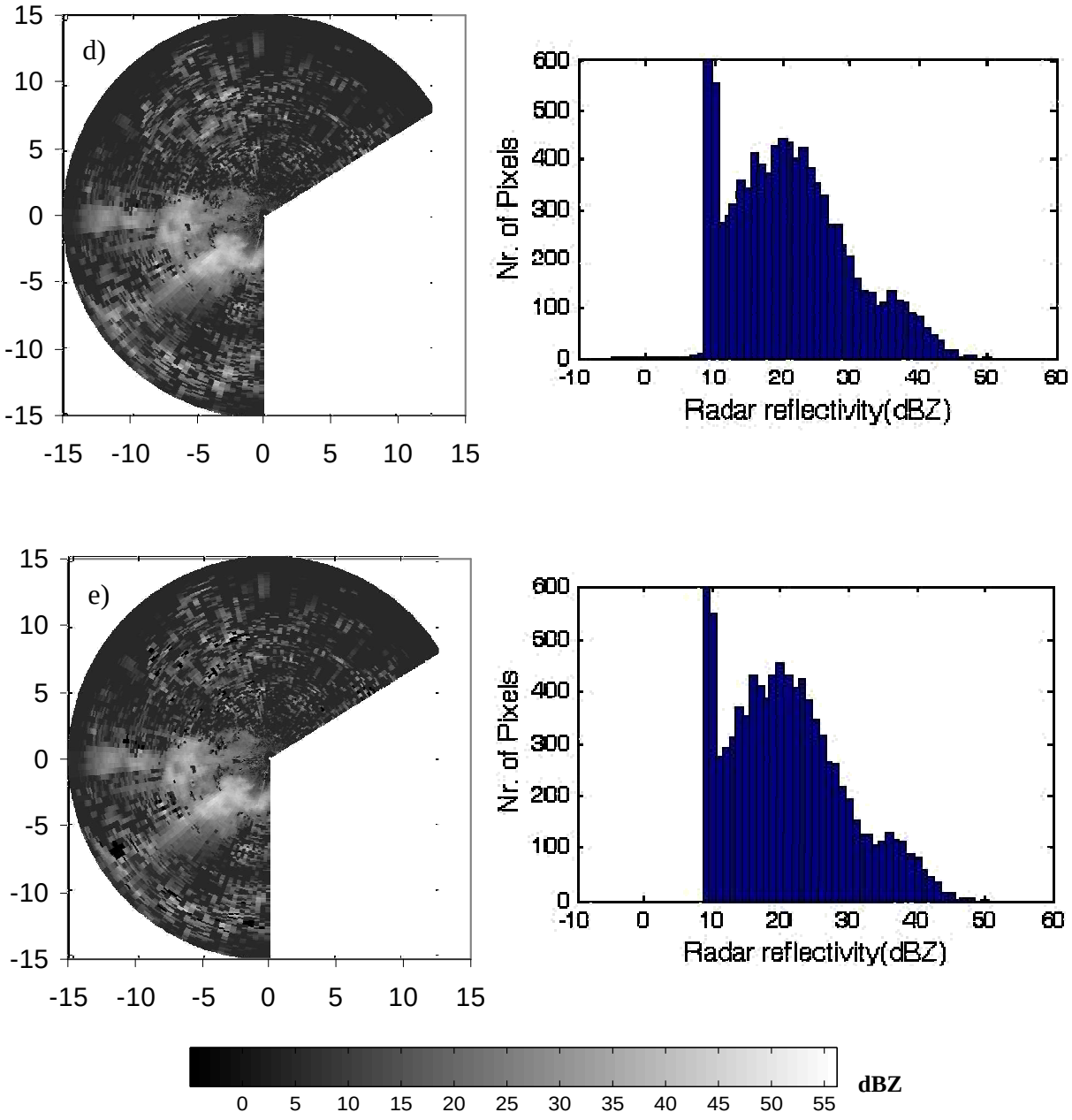

Figure 12 (continued).

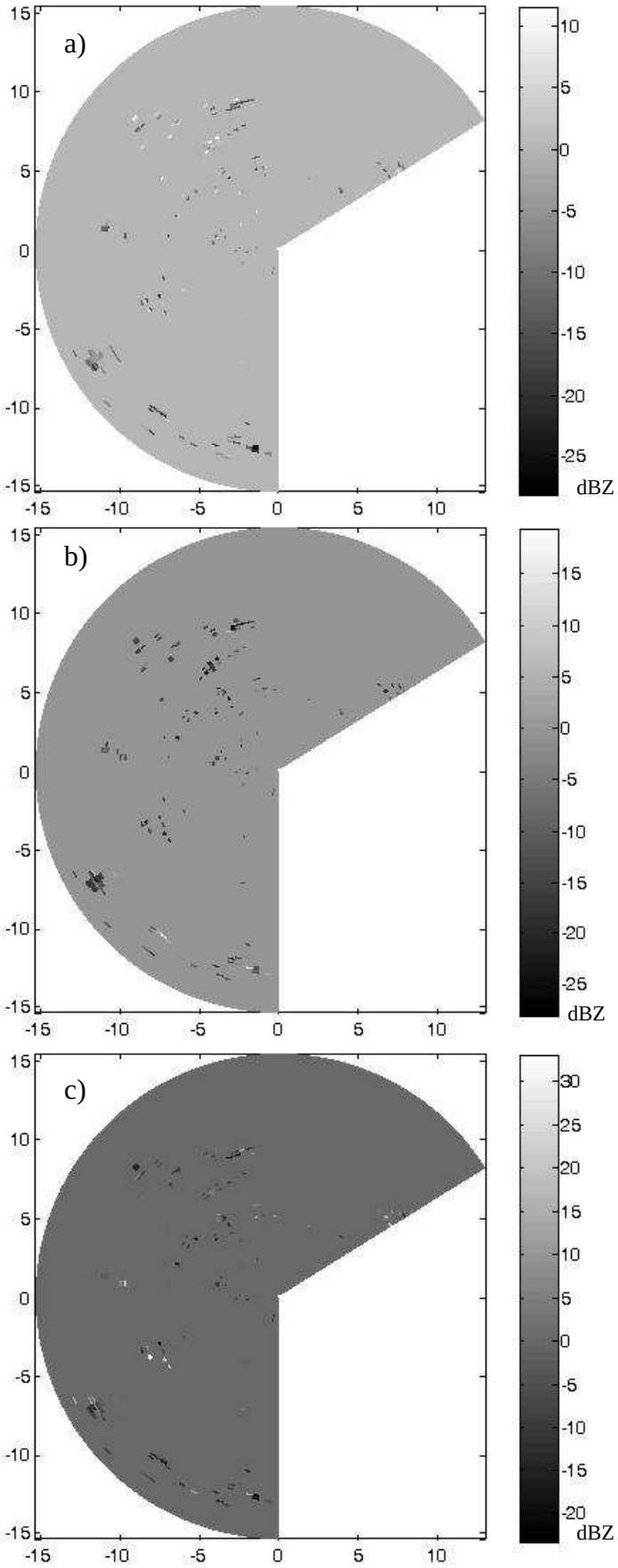

Figure 13: Illustration of differences of two methods of clutter correction in different time on December 19, 1991, a) at 03:09:01, b) at 12:43:14 and c) at 23: 28:16

4.2 Conversion of radar reflectivity factor to rain rate

The next step after elimination of errors is the conversion of radar reflectivity to rain rate in order to compare it with the actual rainfall. As mentioned before, Eq. (7) has been used for this conversion. Figures 14-16 represent the rain rate image derived from the converted fully corrected radar reflectivity data for different time steps and for different methods of clutter correction.

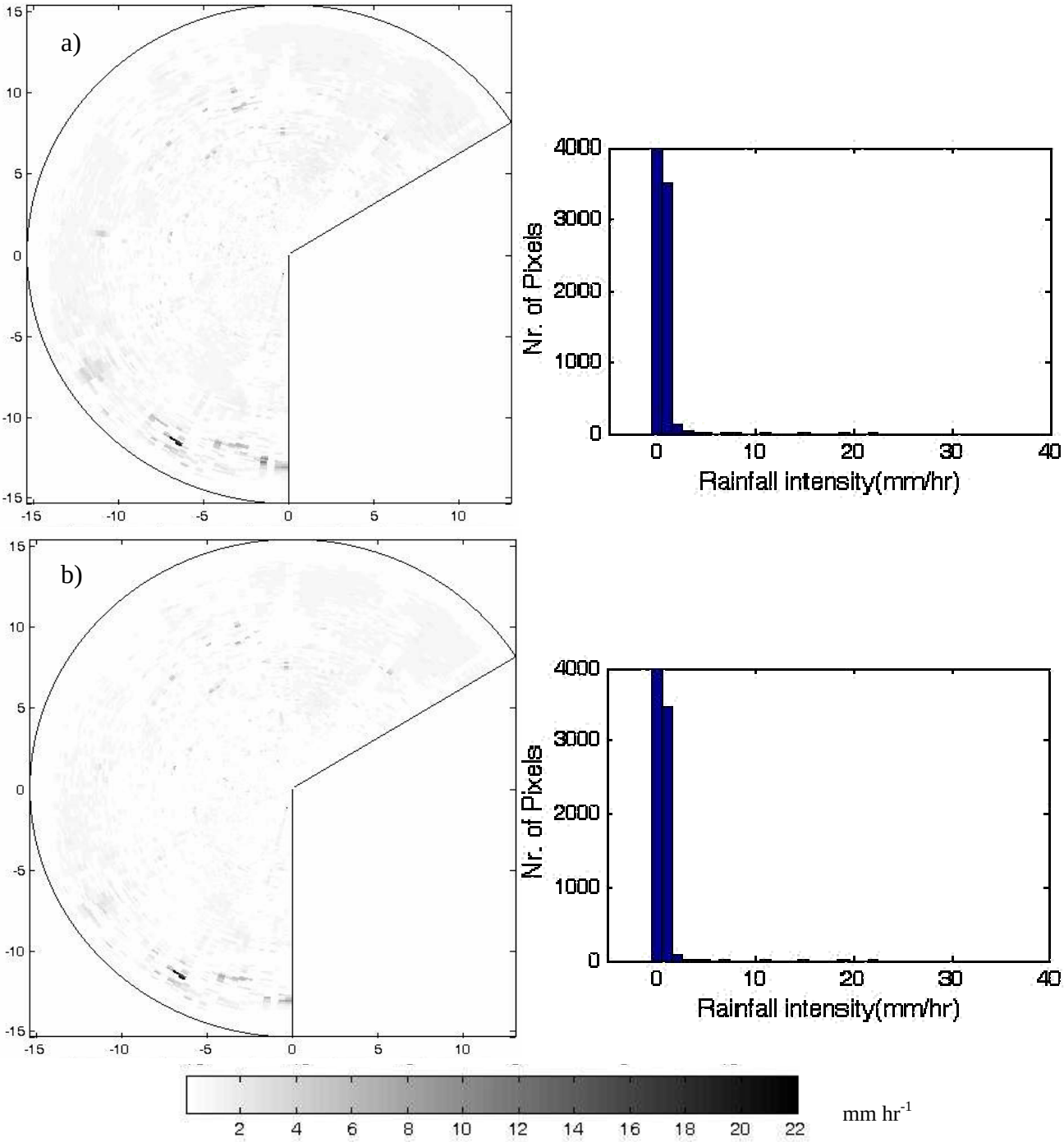

Figure 14: Rain rate image derived from converted clutter and attenuation corrected radar reflectivity data at 03:09:01 on December 19, 1991: a) using the first method of clutter correction and b) using the second method of clutter correction.

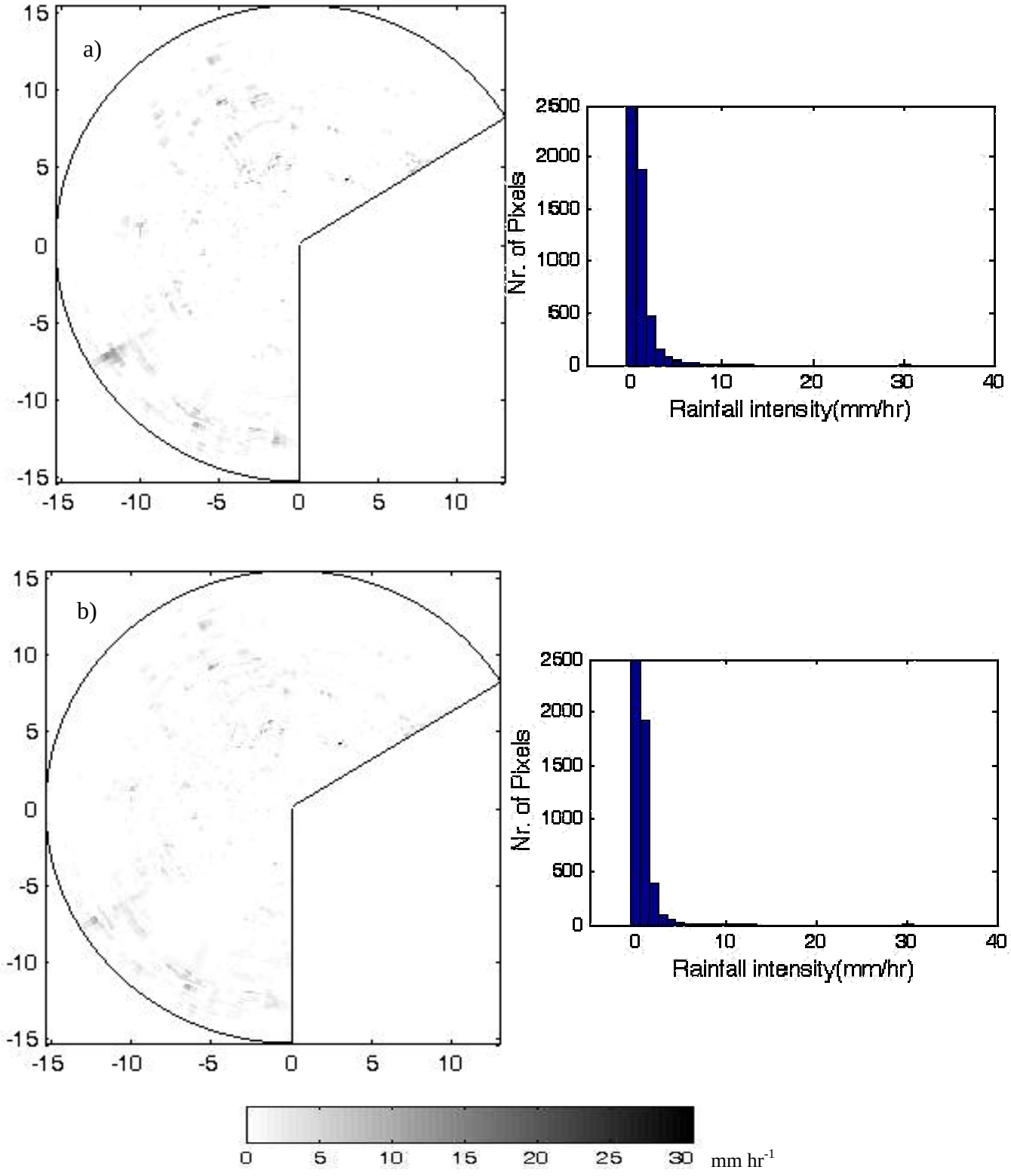

Figure 15: Rain rate image derived from converted clutter and attenuation corrected radar reflectivity data at 12:43:14 on December 19, 1991 a) using the first method of clutter correction and b) using the second method of clutter correction.

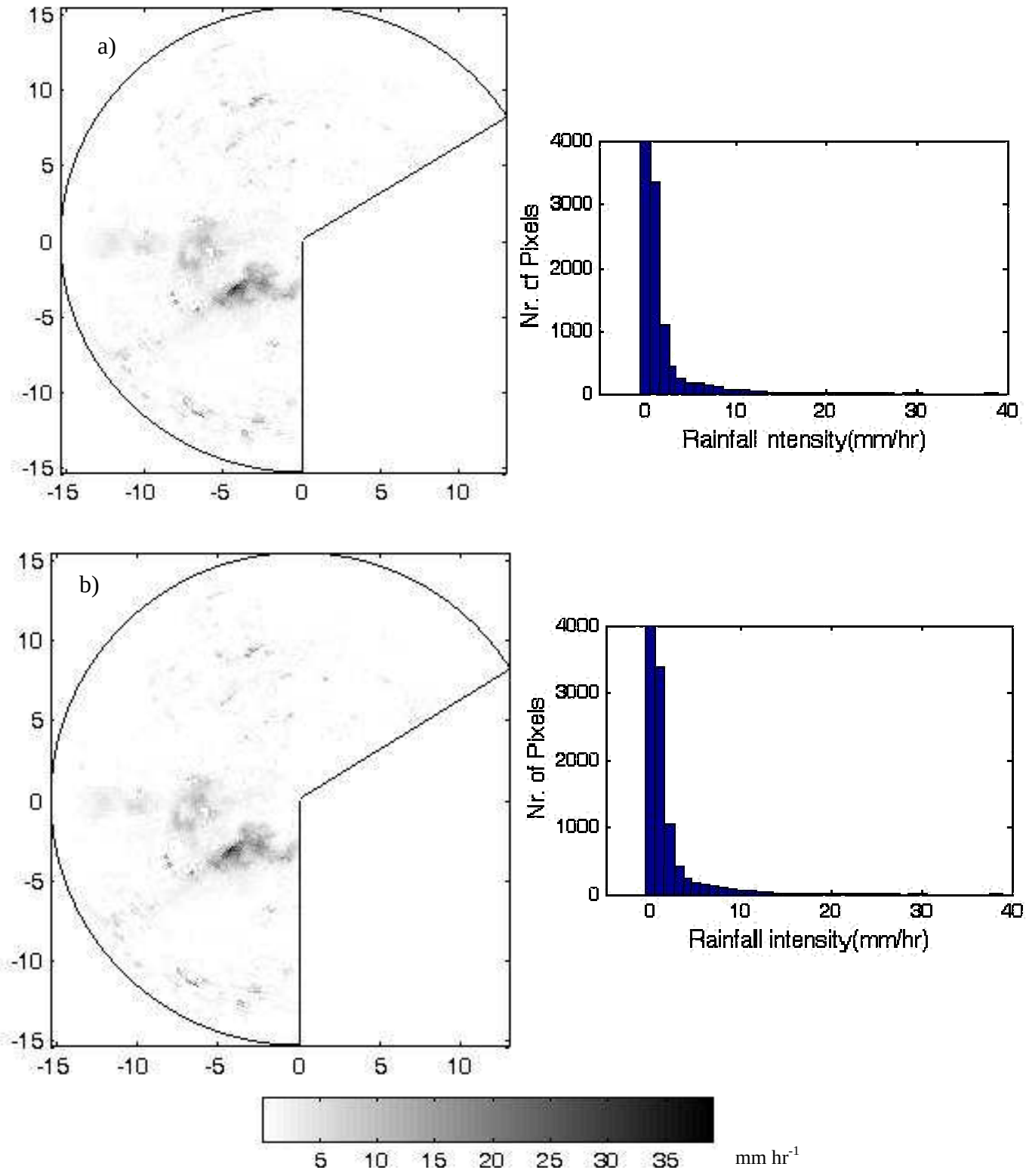

Figure 16: Rain rate image derived from converted clutter and attenuation corrected radar reflectivity data at 23:29:16 on December 19, 1991: a) using the first method of clutter correction and b) using the second method of clutter correction.

As shown in Figs 14-16, there are some points with variable intensity over time and constant position. For instance, at the point in position (-6.5, -11.5) a clutter has been occurred; however none of correction methods couldn't remove the clutter completely. It means that neither method is perfect.

Histograms of images in Figs. 14-16 can be used for comparison of two clutter correction methods. For better insight, differences between two correction methods have been shown in Fig. 17. As shown in this figure, the pixels values in the first method are higher in the most area.

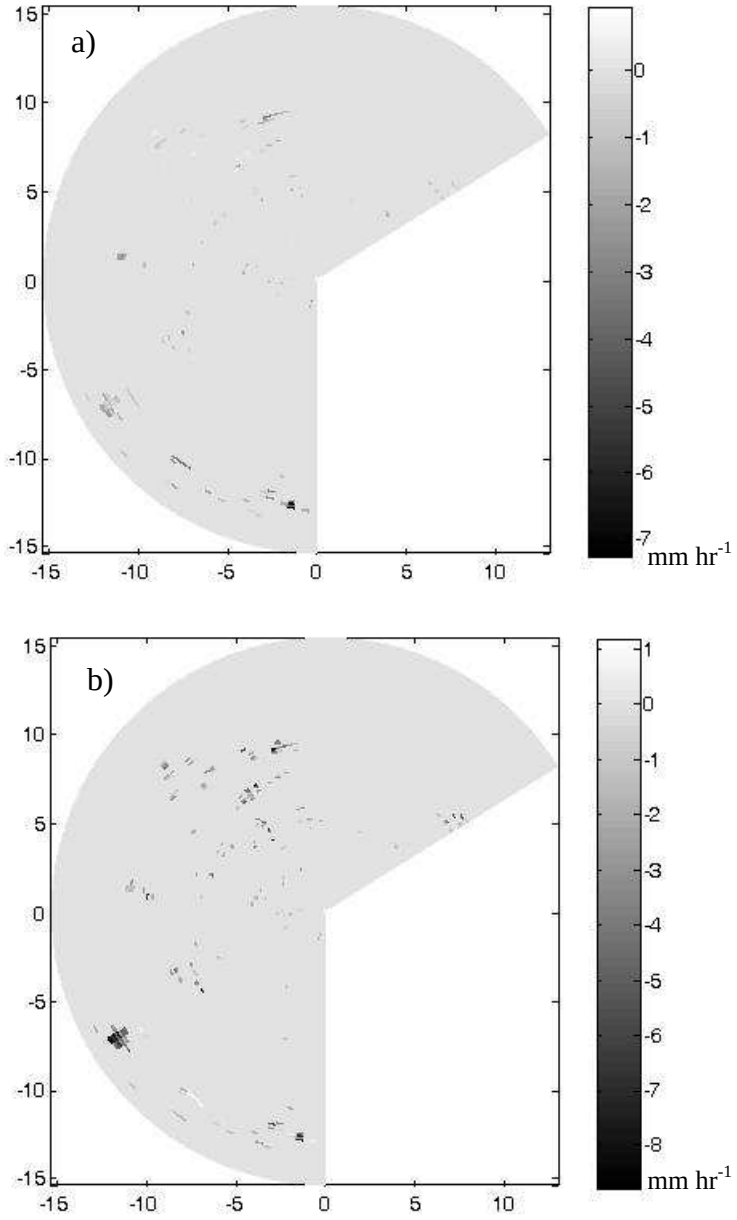

Figure 17: Illustration of differences of two methods of clutter correction in different time on December 19, 1991, a) at 03:09:01, b) at 12:43:14 and c) at 23: 28:16 (continued on next page).

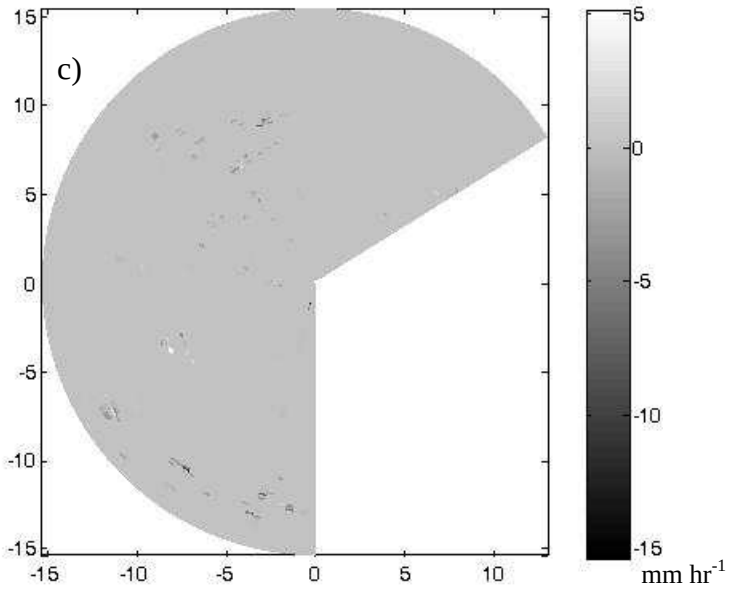

Figure 17 (continued).

4.3 Radar- gauge comparison over the study area

In order to assess the uncertainty in rainfall estimation, rainfall intensities estimated from the X-band weather radar have been compared against rain gauges. Radar data from the pixels above the gauges have been used for this purpose.

Figures 18-21 show the resulting rain rate time series for SOLIDAR as compared to the rain gauges. Comparison of radar rainfall estimates with the data from the 4 gauges in the study area shows that the radar follows the general trend in the rain gauge measurements. However in some times there are some differences between radar estimation and data that rain gauges recorded. This might be attributed to insufficient attenuation correction and calibration error.

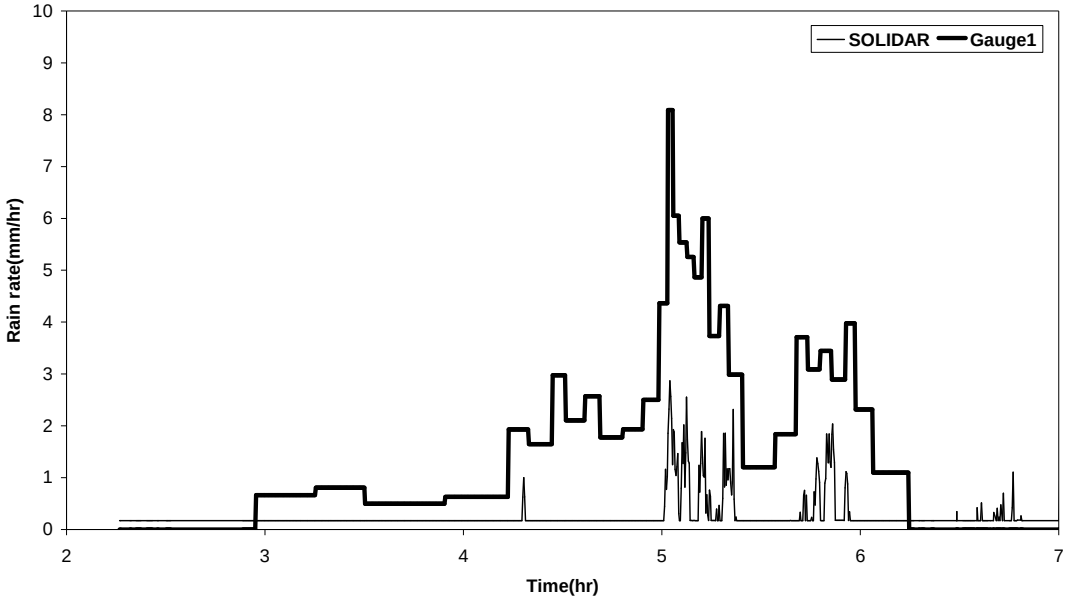

Figure 18: Time series of rain rates as measured by radar and rain gauge Nr.1 on December 19, 1991.

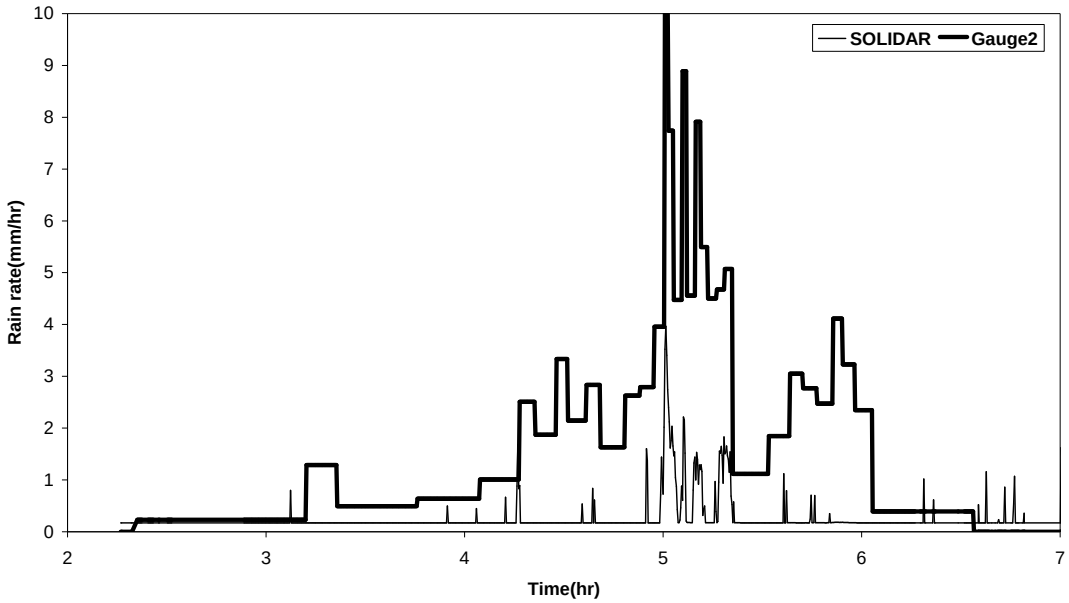

Figure 19: Time series of rain rates as measured by radar and rain gauge Nr.2 on December 19, 1991.

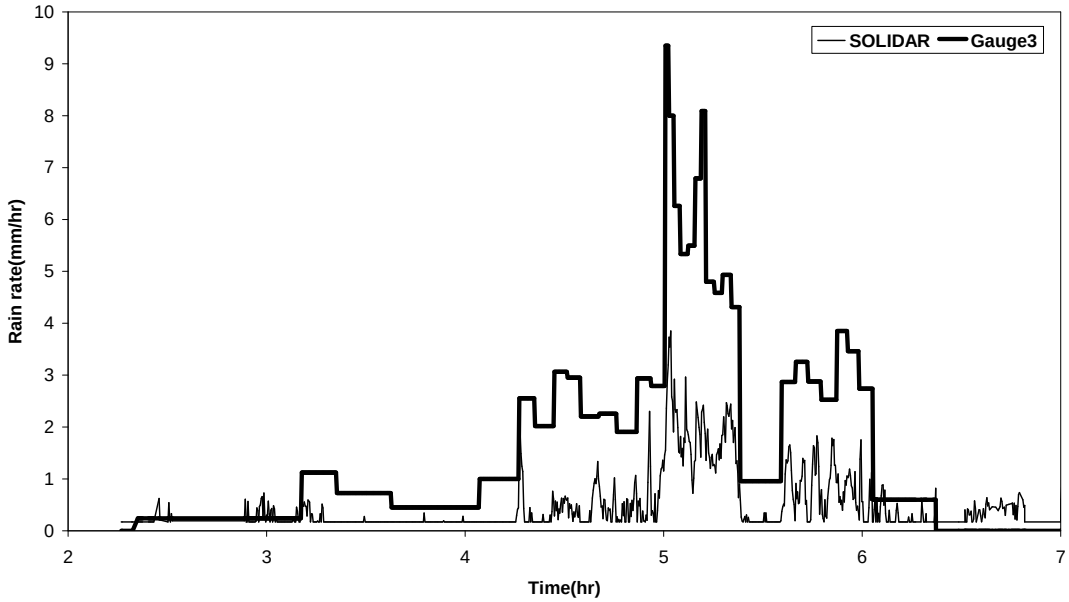

Figure 20: Time series of rain rates as measured by radar and rain gauge Nr.3 on December 19, 1991.

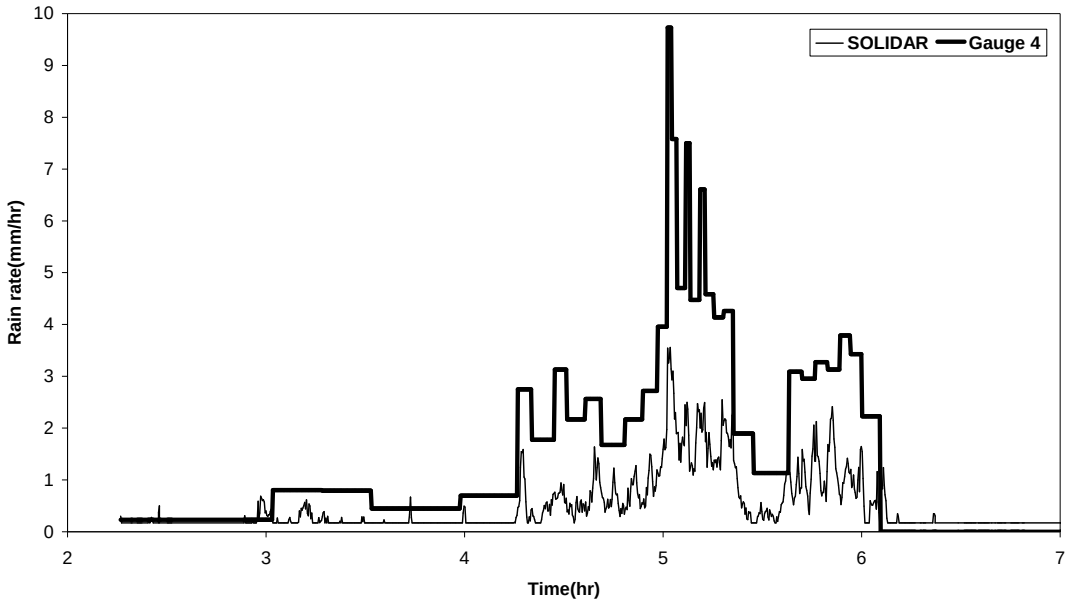

Figure 21: Time series of rain rates as measured by radar and rain gauge Nr.4 on December 19, 1991.

Calibration errors may greatly affect the corresponding rainfall estimates. Therefore an extra correction factor (2.28, corresponding to 6.2 dB) has been applied to the radar estimation. This correction factor has been reported by the radar operator. Figs. 22-25 show that the results after the calibration were greatly improved. A closer look at the radar estimation indicated that the radar has a limitation in recording at low ranges. The noise level of the radar is 9 dB. With the 6.2 dB calibration factor this corresponds to a minimum rainfall intensity of 0.39 mm h^{-1}.

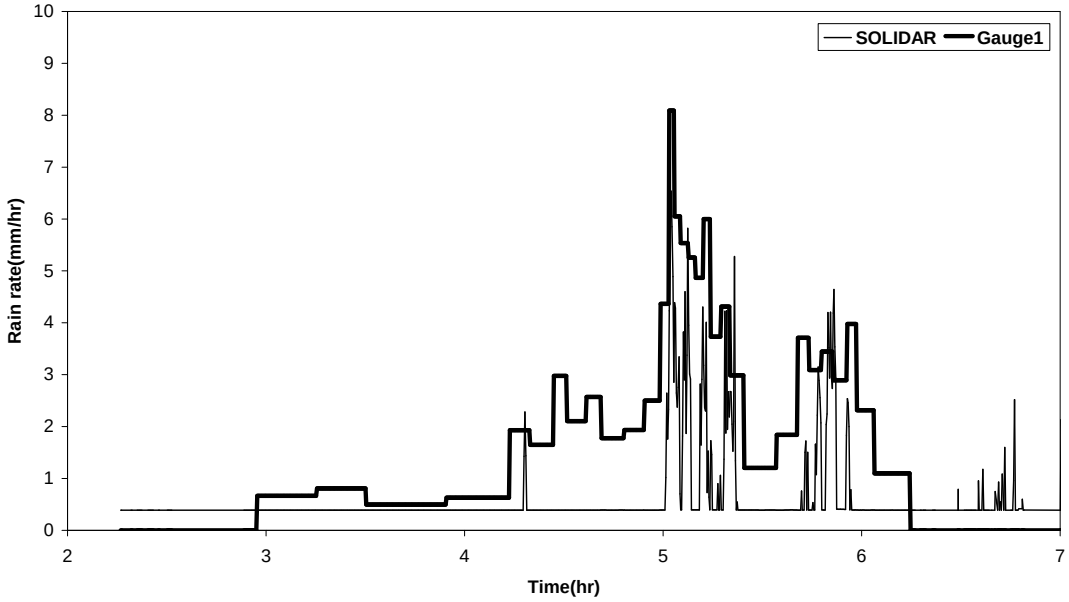

Figure 22: Time series of rain rates as measured by radar (corrected for the calibration error) and rain gauge Nr.1 on December 19, 1991.

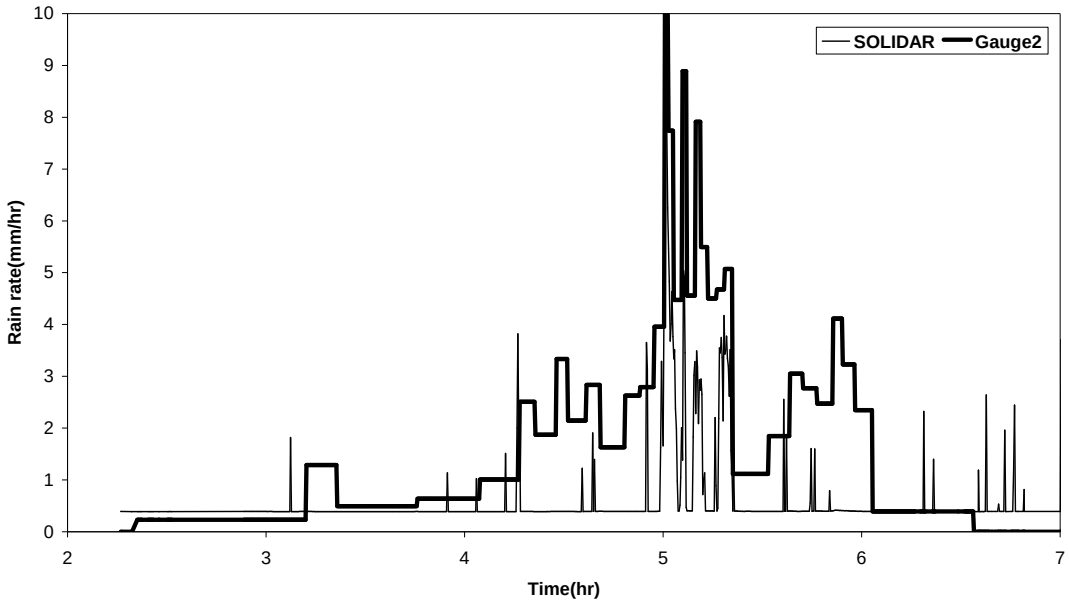

Figure 23: Time series of rain rates as measured by radar (corrected for the calibration error) and rain gauge Nr.2 on December 19, 1991.

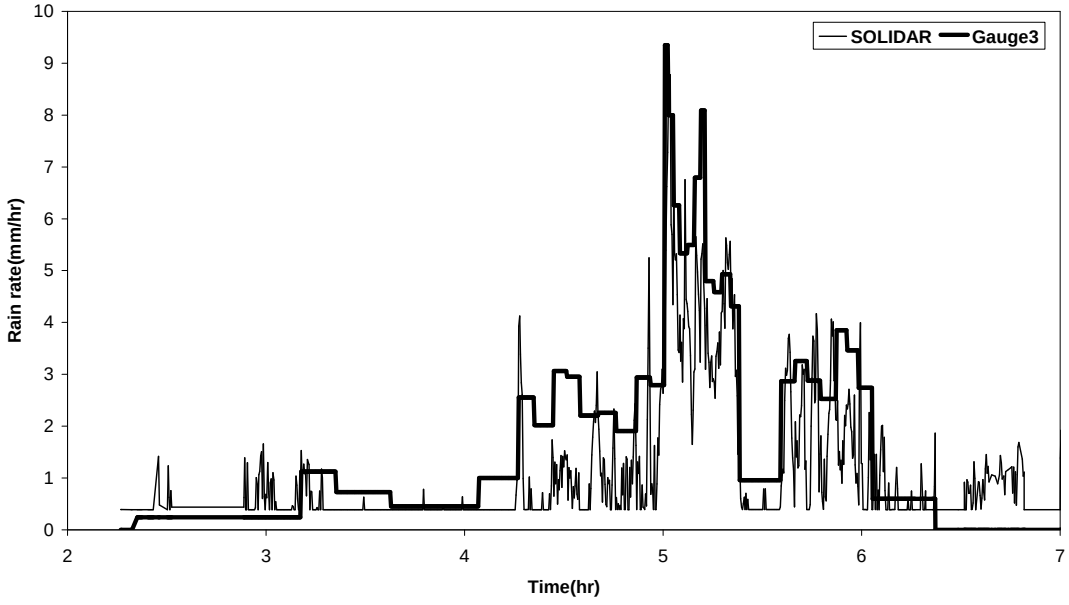

Figure 24: Time series of rain rates as measured by radar (corrected for the calibration error) and rain gauge Nr.3 on December 19, 1991.

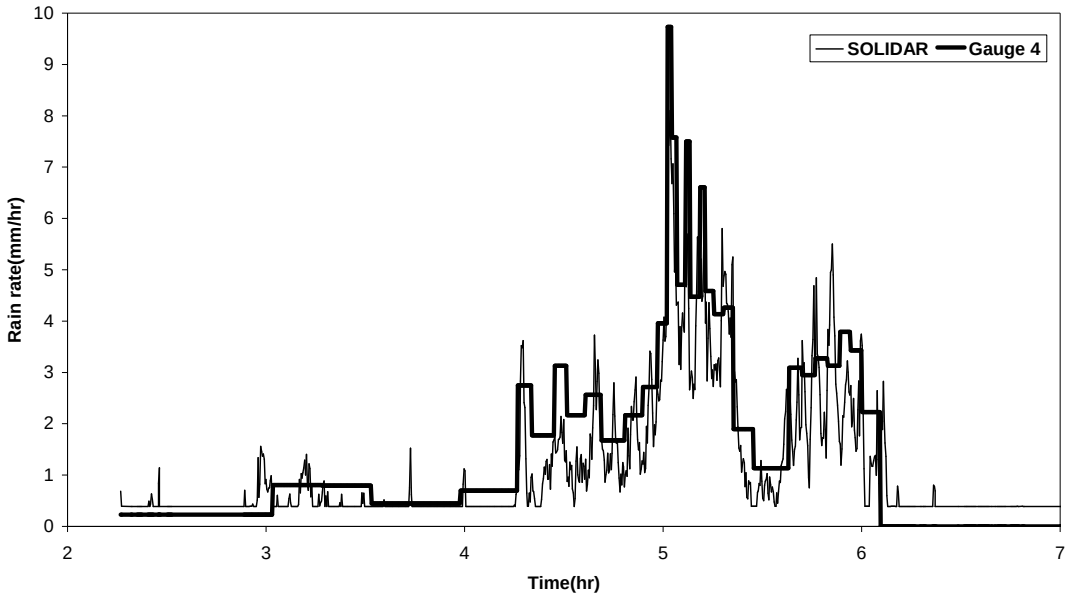

Figure 25: Time series of rain rates as measured by radar (corrected for the calibration error) and rain gauge Nr.4 on December 19, 1991.

It can be seen in figs. 26-29 that at all locations, the radar estimates of the total rainfall amounts before and after calibration are still lower than the corresponding rain gauge measurements. The mean bias error of these estimations confirms this (see also Table 4). As can be seen the radar follows the general trend in the rain gauge measurements.

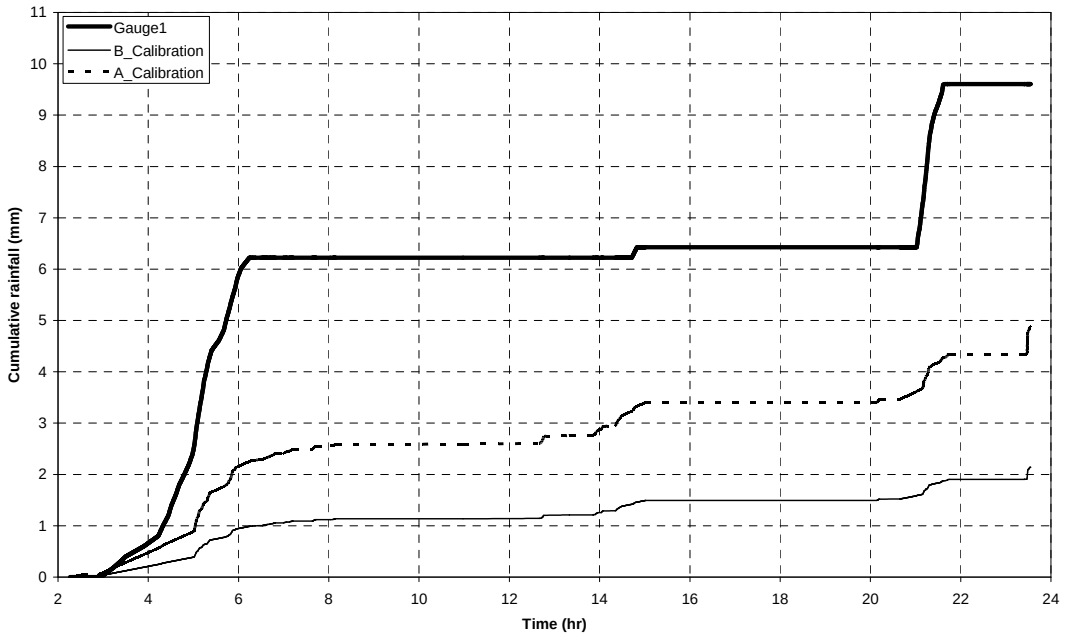

Figure 26: The cumulative rainfall against time for un-calibrated and calibrated radar and rain gauge Nr.1 on December 19, 1991.

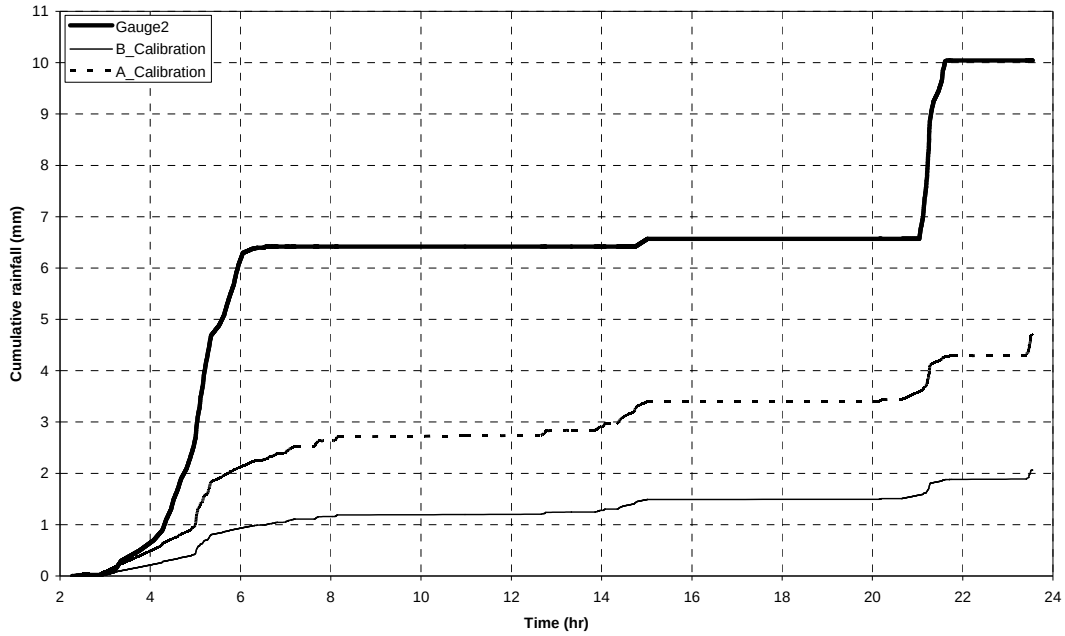

Figure 27: The cumulative rainfall against time for un-calibrated and calibrated radar and rain gauge Nr.2 on December 19, 1991.

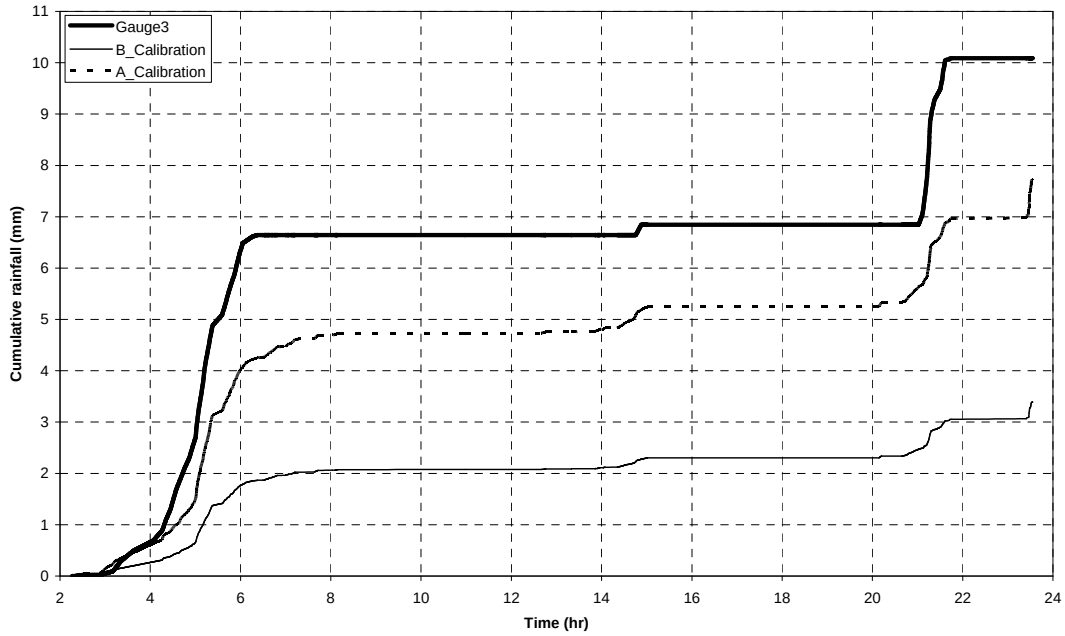

Figure 28: The cumulative rainfall against time for un-calibrated and calibrated radar and rain gauge Nr.3 on December 19, 1991.

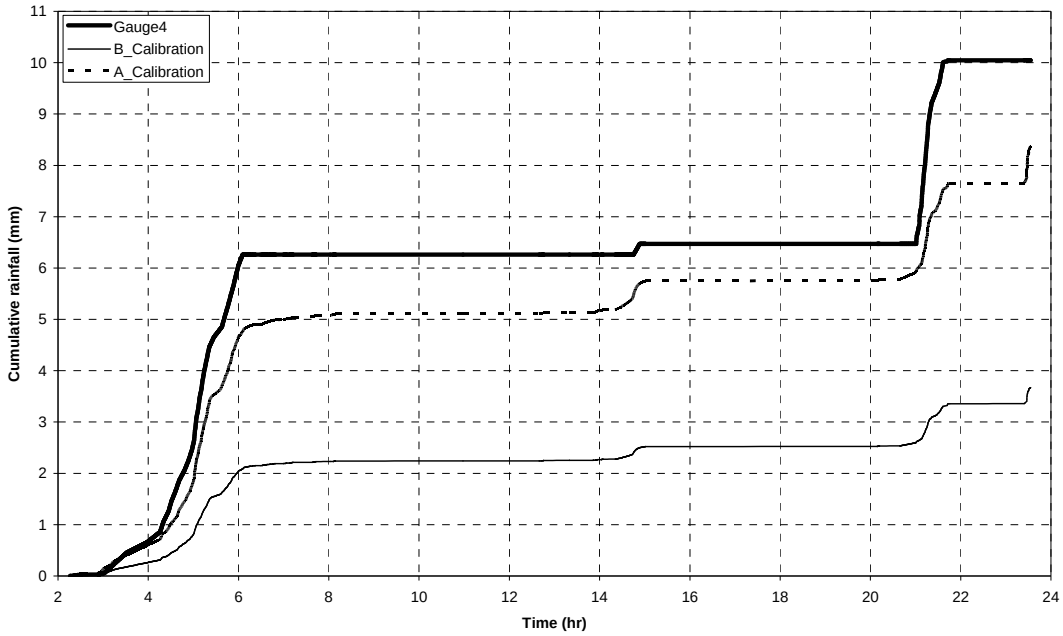

Figure 29: The cumulative rainfall against time for un-calibrated and calibrated radar and rain gauge Nr.4 on December 19, 1991.

Table 4 gives a summary of the statistics of the time series in terms of the mean bias errors *(MBE)*, the root mean square errors *(RMSE)* and Table 5 shows the correlation coefficients (r).

As can be seen in fig. 9 the radar pixels above the rain gauges are not affected by clutter. Therefore in Table 4 the results of the statistical analysis of the time series of rain rates as measured by the radar and rain gauges at different locations are only shown for the second method of clutter correction. There is no significant difference between the rain rates estimated by the radar for the two methods of clutter correction due to position of the rain gauges.

As can be expected these statistics confirm the previous graphs in the sense that the estimated data after calibration has been improved.

Since the values of the correlation coefficient after calibration at the location of each rain gauge are low and the rain rates estimated by radar are not very important when there is no rain, the radar estimations that correspond to the zero values of the rain gauges have not been taken into account in the calculation of the correlation coefficient. The result has been presented in Table 5. After removal of the zero values, the coefficient of correlation (r) has been improved and its value increased. The r-values of 0.7 show that the radar at least follows the trend of rainfall intensities.

Table 4: Results of statistical analysis of time series rain rates as measured by radars and rain gauges at different locations. *MBE:* mean bias error [mm h^{-1}]; *RMSE:* root mean square error [mm h^{-1}].

position	***data***	***MBE***	***RMSE***
Gauge1	original Data	-1.22	2.34
	calibrated Data	-0.77	2.35
Gauge 2	original Data	-1.31	2.76
	calibrated Data	-0.87	2.51
Gauge 3	original Data	-1.10	2.37
	calibrated Data	-0.39	2.15
Gauge 4	original Data	-1.05	2.32
	calibrated Data	-0.28	2.12

Table 5: Coefficient of correlation, r [-].

	Original data	*After removal of zero values*
Gauge 1	0.22	0.53
Gauge 2	0.44	0.7
Gauge 3	0.53	0.77
Gauge 4	0.53	0.71

Chapter 5

Conclusions and Recommendations

5.1 Conclusions

To answer all the research questions, a study of the use of high-resolution X-band weather surveillance radar for areal rainfall estimation, based on the case of the region around Delft in the south-western part of The Netherlands, is carried out in three main parts: preprocessing of raw data, conversion of radar reflectivity to rain rate and comparison of radar estimation against rain gauges in study area. In this report a description of the solid-state X-band weather radar SOLIDAR has been given as well. The corresponding answers to each research objective are given as follows.

- **How to improve rainfall estimation using weather radar?**

To improve rainfall estimation by SOLIDAR, radar measurements have been firstly corrected for attenuation and ground clutter. Then, the rain rates have been obtained by using a relevant power-law relationship between radar reflectivity and rain rate. In order to suppress clutter errors, firstly a ground clutter map has been established and clutter errors have been eliminated by using two separate methods. A comparison between these two different methods shows that the second method of correction is

better than the first one. The first method is based on the intensity of ground clutter map, which may change with time, whereas the second method is based only on the location of the clutter. Of course there is no evidence to improved that the second method how much is better than first method, because of lack of rain gauge data at clutter position.

Attenuation correction is an important step for quantitative rain estimation using X-band weather. Analyses have shown that for low rain- rates the effects of attenuation are small but at high rain rates, it affects the radar measurements.

- **How to assess the uncertainty in rainfall estimation?**

Evaluating the accuracy of rainfall- rates estimated using radar data is a major step in this process. In order to assess the uncertainty in estimation, the results have been compared with rain gauges data in the study area. Time series of rainfall rate and cumulative rainfall have been analyzed for both radar estimation and gauges. MBE, RMSE and correlation coefficient have been calculated.

According to the time series graphs, comparison of radar rainfall estimates with the data from the 4 gauges in study area shows that the radar follows the general trend of the rain gauge measurements. But at all locations, the radar estimates of the total rainfall amount values are lower than the corresponding rain gauge measurements. The cumulative rainfall graphs and MBE confirm this.

The causes of the underestimation can be manifold: the SOLIDAR radar data have been corrected for ground clutter and attenuation, but other important error sources like a non- optimized Z-R relationship and a poor electronic calibration of the radar may have had an impact on the rainfall estimation.

Errors caused by temporal sampling, spatial sampling, height sampling and variation in the Z-R relationship may also have caused the discrepancy. They can not be easily removed or reduced.

The advantage of radar data compared to rain gauge data is increased time resolution and spatial coverage. Also radar data can provide much more insight in the spatial variation of rainfall and, therefore, in uncertainties in the areal precipitation estimates

obtained from rain gauges. As can be seen in this report radar data are available for the entire area but in this area, only 4 rain gauges had been installed.

In general, the result shows that the radar measurements need to be calibrated and corrected for errors. Because some of the errors cannot be easily removed or reduced, they will affect the accuracy of result. When corrections are applied, results are comparable to the rain gauge measurement. However, in this respect one question remains: can a tipping bucket rain gauge measurement be assumed to represent the ground truth or not?

5.2. Recommendations:

It is recommended that further work may focus on:

- A more extended data set, including the uncorrected radar data in order to improve the detection of attenuation affecting the radar and the ground clutter, using an improved algorithm.
- Install more rain gauges in the study area especially in locations affected by clutter.
- Using S-band radar as a non-attenuated reference. With this data the Z-R and *k*-Z relationship can be determined more accurately and the accuracy of rainfall rate estimations is increased.
- Using dual polarization radar. Sensitivity of this kind of radar to the DSD is less than for single polarization radar (Park et al., 2004, Jordan et al., 2004). Signals returned by the horizontal and vertical polarized beams provide additional parameters that can be combined into a more robust multi-parameter estimate of rainfall intensity.

References:

Battan, L. J., 1973: Radar Observation of the Atmosphere, *The University of Chicago Press*, 324 pp.

Bell, V. A. and Moore, R. J., 1998: A grid-based distributed flood forecasting model for use with weather radar data: Part 2. Case studies, *Hydrol. Earth Syst. Sci.*, 2, 283–298.

Berne, A. and R. Uijlenhoet, 2006: Quantitative analysis of X-band weather radar attenuation correction accuracy, *Nat. Hazards Earth Syst. Sci*., 6, 419–425.

Borga, M. and S. Fattorelli, 2002: Use of Radar Rainfall Estimates for Stream flow Simulation an Assessment of Predictive Uncertainty, Available online at: (http://www.hrwallingford.co.uk/Mitch/Workshop2/Papers/Borga.pdf)

Borga, M. and F. Tonelli, 2002: A Baysian approach to assessment of uncertainty in radar rainfall estimates, Water Resources Research, 38(11): 1226.

Calheiros, R. V. and I. Zawadzki, 1987: Reflectivity rain-rate relationships for radar hydrology in Brazil, Appl. Meteorol., 26, 118–132.

Chrisman, J. N., D. M. Rinderknecht, R. S. Hamilton, 1995: WSR-88D Clutter Suppression and Its Impact On Meteorological Data Interpretation, WSR-88D Operational Support Facility Operations Trainig Branch Norman, OK 73072.

Chua, S. H. and R. F. Bras, 1982: Optimal estimation of mean areal precipitation in regions of orographic influences, J. Hydrol., 57, 713–728.

Cluckie, I. D., M. A. R. Ramirez, T. Zawislak and W. Szalinska, 2005: Preliminary Study of Vertical Radar Reflectivity Profiles over the Orda Basin, *international conference "Innovation, advance and implementation of flood forecasting technology"*, Tromsø, Norway.

Collier, C. G., 1996: Applications of weather radar systems: A guide to uses of radar data in meteorology and hydrology, *John Wiley & Sons*, New York, USA.

Collinge, V. K. and C. Kirby, 1987: Weather radar and flood forecasting, John Wiley & Sons, Great Britain, England,

Gabella, M. and R. Notarpietro, 2002: Ground clutter characterization and elimination in mountainous terrain, *Proceedings of the 2nd ERAD conference, Delft, The Netherlands*, 305–311.

Gerstner, T., D. Meetschen, S. Crewell, M. Griebel, C. Simmer, 2002: Case Study: Visualization of Local Rainfall from Weather Radar Measurements, *Joint EUROGRAPHICS - IEEE TCVG Symposium on Visualization*, 1-7.

Gray, W and H. Larsen, 2004: Radar Rainfall Estimation in the New Zealand Context, *Sixth International Symposium on Hydrological Applications of Weather Radar*, Melbourne, Australia.

Harrison, D. L., S. J. Driscoll, and M. Kitchen (2000) Improving precipitation estimates from weather radar using quality control and correction techniques. *Meteorol. Appl*., 6:135-144.

Heggeler, M. ten, 2004: Hydrological Modeling and Areal Average Rainfall Estimates of the Ourthe Catchment Derived from the Wideumont Weather Radar and Precipitation Gauges, *MSc thesis*, Wageningen University, Netherlands.

Hitschfeld, W. and J. Bordan, 1954: Errors Inherent in the Radar Measurement of Rainfall at Attenuating Wavelengths, *J. Meteorology*, 11, 58–67.

Jordan, P.W., 2000: Errors in radar measurements of rainfall – effects on flood forecasting, Available online at: (http://www.smec.com.au/media/papers/hydro200.pdf)

Jordan, P.W., A. Seed, P. May and T. Keenan, 2004: Evaluation of Dual Polarization Radar for Rainfall-Runoff Modeling – A Case Study in Sydney, Australia, *Sixth International Symposium on Hydrological Applications of Weather Radar*, Melbourne, Australia.

Krajewski, W. F. and J. A. Smith, 2002: Radar hydrology: rainfall estimation, *Adv. Water Resour*., 25(8), 1387–1394.

Ligthart, L.P., L.R. Nieuwkerk, 1990: An X-band Solid- State FM-CW Weather Radar, *IEE Proceedings*, 137, 418-426.

Linsley, R. K., M. A. Kohler and J. L. H. Paulhus, 1988: Hydrology for engineers, *McGraw-Hill*, London, UK.

Lombardo, F., F. Napolitano, F. Russo, G. Scialanga, L. Baldini, and E. Gorgucci, 2006: Rainfall estimation and ground clutter rejection with dual polarization weather radar, *Advances in Geosciences*, 7, 127–130.

Lopez, V., F. Napolitano, and F. Russo, 2005: Calibration of a rainfall-runoff model using radar and rain gauge data, *Advances in Geosciences*, 2, 41–46.

Marshall, J. S. and W. Mck. Palmer, 1948: The distribution of raindrops with size, *J. Meteorol.*, 165–166.

Marzoug, M., P. Amayenc, 1994: A Class of Single- and Dual- Frequency Algorithms for Rain-Rate Profiling from a Spaceborne Radar. Part I: Principle and Tests from Numerical Simulations, *Journal of Atmospheric and Oceanic Technology*, 11, 1480- 1506.

Matrosov, S. Y., K. A. Clark, B.E. Martner and A. Tokay, 2002: X-Band Polarimetric Radar Measurements of Rainfall, *J. Appl. Meteorol.*, 41, 941-952.

Osrodka, K., A. Jurczyk, and J. Szturc, 2004: Effects of radar data improvements on hydrological modeling, *Proceedings of 3rd ERAD conference, Visby, Sweden*, 528–530.

Park, S.G., M. Maki, K. Iwanami, R. Misumi and V. N. Bringi, 2004: Correction of Radar Reflectivity and Differential Reflectivity for Rain Attenuation and Estimation of Rainfall at X-band Wavelength, *Sixth International Symposium on Hydrological Applications of Weather Radar*, Melbourne, Australia.

Perez, M. A. and I. Zawadzki, 2003: S- and X-band dual-wavelength radars revisited, available online at: (http://ams.confex.com/ams/pdfpapers/63432.pdf)

Piman, T., M. S. Babel, A. D. Gupta, and S. Weesakul, 2007: Development of a window correlation matching method for improved radar rainfall estimation, *Hydrol. Earth Syst. Sci. Discuss.*, 4, 523–554.

Rahimi, A. R., A. R. Holt, G. J. G. Upton, S. Krämer, A. Redder and H-R Verworn, 2006: Attenuation Calibration of an X-band Weather Radar using a Microwave Link, *Journal of Atmospheric and Oceanic Technology* , 23, 395-405.

Rosenfeld, D., D. B. Wolff, and D. Atlas, 1993: General probability-matched relations between radar reflectivity and rain rate, *J. Appl. Meteorol.*, 32, 50–72.

Stagliano, Jr., J. J. , J. Helvin, J. L. Alford, and D. Nelson, Phase Noise, Coherency and Clutter Suppression, available online at: http://ams.confex.com/ams/pdfpapers/95615.pdf

Sun, X., R. G. Mein, T. D. Keenan, and J. F. Elliott, 2000: Flood estimation using radar and rain gauge Rata, *J. Hydrol.*, 239, 4–18.

Tilford, K A , N. I. Fox and C. G. Collier, 2002: Application of weather radar data for urban hydrology, *Meteorol. Appl*. 9, 95–104.

Uijlenhoet, R., 1992: Determination of Areal Rainfall from Separate and Combined use of Different Types of Radars and a Rain Gauge Network: An X-band FM-CW Radar Perspective, *2nd International Symposium on Hydrological Applications of Weather Radar*, Hanover, Germany.

Uijlenhoet, R., 2001: Raindrop size distributions and radar reflectivity–rain rate relationships for radar hydrology. *Hydrology and Earth System Sciences*, 5, 615–627.

Uijlenhoet, R., J.N.M. Stricker and H.W.J Russchenberg, 1997: Application of X- and S-Band Radars for Rain Rate Estimation over an Urban Area, *Phys. Chem. Earth*, 22, 259-264.

Uijlenhoet, R., S.H. van der Wielen and A. Berne, 2006: Uncertainties in rainfall retrievals from ground-based weather radar: overview, case study, and simulation experiment, *Hydrol. Earth Syst. Sci. Discuss*., 3, 2385–2436.

Vaes, G., P. Willems, and J. Berlamont, 2001: Rainfall input requirements for hydrological calculations, *Urban Water*, 3, 107–112.

Wesson, S. M. and G. G. S. Pegram, 2006: Improved radar rainfall estimation at ground level, *Nat. Hazards Earth Syst. Sci.*, 6, 323–342.

Wilson, J., and E. Brandes, 1979: Radar Measurement of Rainfall- A Summary. *Bulletin of American Meteorological Society*. 60(9): 1048-58.

Windsor, M., 2002, Statistical Comparison of Radar Estimated Rainfall Data vs. Rain Gauge Data, available online at: (http://www.utsa.edu/LRSG/Teaching/EES5053/Projects/ Matt%20 Windsor.pdf)